

N-Benzyl-4-((heteroaryl)methyl)benzamides: A New Class of Direct NADH-Dependent 2-trans Enoyl-Acyl Carrier Protein Reductase (InhA) Inhibitors with Antitubercular Activity

Ana Guardia,^{*[a]} Gulcin Gulten,^[b] Raquel Fernandez,^[a] Jesus Gómez,^[a] Feng Wang,^[c] Maire Convery,^[d] Delia Blanco,^[a] María Martínez,^[a] Esther Pérez-Herrán,^[a] Marta Alonso,^[a] Fátima Ortega,^[a] Joaquín Rullás,^[a] David Calvo,^[e] Lydia Mata,^[e] Robert Young,^[d] James C. Sacchettini,^[b] Alfonso Mendoza-Losana,^[a] Modesto Remuiñán,^[a] Lluís Ballell Pages,^[a] and Julia Castro-Pichel^[a]

Isoniazid (INH) remains one of the cornerstones of antitubercular chemotherapy for drug-sensitive strains of *M. tuberculosis* bacteria. However, the increasing prevalence of multidrug-resistant (MDR) and extensively drug-resistant (XDR) strains containing mutations in the KatG enzyme, which is responsible for the activation of INH into its antitubercular form, have rendered this drug of little or no use in many cases of drug-resistant tuberculosis. Presented herein is a novel family of antitubercular direct NADH-dependent 2-trans enoyl-acyl carrier protein reductase (InhA) inhibitors based on an N-benzyl-4-((heteroaryl)methyl)benzamide template; unlike INH, these do not re-

quire prior activation by KatG. Given their direct InhA target engagement, these compounds should be able to circumvent KatG-related resistance in the clinic. The lead molecules were shown to be potent inhibitors of InhA and showed activity against *M. tuberculosis* bacteria. This new family of inhibitors was found to be chemically tractable, as exemplified by the facile synthesis of analogues and the establishment of structure-activity relationships. Furthermore, a co-crystal structure of the initial hit with the enzyme is disclosed, providing valuable information toward the design of new InhA inhibitors for the treatment of MDR/XDR tuberculosis.

Introduction

Tuberculosis (TB) continues to be a global threat, with an additional nine million people infected—and one and a half million still dying from the disease—each year.^[1] The increasing prevalence of multidrug-resistant (MDR)^[2–6] and extensively drug-re-

sistant (XDR)^[7,8] TB strains, along with the commonly encountered co-infection in HIV patients and lack of adherence to multidrug frontline treatment regimes are factors that contribute to this pandemic. Despite the proven efficacy of *Directly Observed Treatment Short course* (DOTS),^[9] which has a cure rate of >90%, the development of new drugs with novel modes of action for the treatment of TB remains an urgent unmet medical need. A shortened treatment regime for both drug-sensitive and MDR/XDR TB would have a significant impact. The urgency for new treatments is perhaps embodied in the profile of bedaquiline,^[10] which is the first new antimycobacterial drug to be approved by the US Food and Drug Administration (FDA) in over 40 years; it was approved at the end of 2012. Bedaquiline acts by the novel mechanism of inhibiting mycobacterial adenosine 5'-triphosphate (ATP) synthase, with good clinical efficacy against multiple resistant strains. Although it has saved lives, it was approved with a black-box warning, highlighting the possibility of severe cardiovascular side effects.^[10]

The well-validated drug target InhA acts as an NADH-dependent 2-trans enoyl-acyl carrier protein (ACP) reductase within the type II fatty acid synthase (FASII) pathway in *M. tuberculosis*^[11] and is the primary target of the frontline antitubercular drug isoniazid (INH).^[12–14] INH is activated within the mycobacterium by the catalase-peroxidase enzyme KatG, forming the

[a] A. Guardia, Dr. R. Fernandez, J. Gómez, D. Blanco, M. Martínez, Dr. E. Pérez-Herrán, M. Alonso, Dr. F. Ortega, Dr. J. Rullás, Dr. A. Mendoza-Losana, Dr. M. Remuiñán, Dr. L. Ballell Pages, Dr. J. Castro-Pichel
Diseases of the Developing World, GlaxoSmithKline
Severo Ochoa 2, 28760 Tres Cantos, Madrid (Spain)
E-mail: ana.a.guardia@gsk.com

[b] Dr. G. Gulten, Prof. J. C. Sacchettini
Department of Biochemistry and Biophysics, Texas A&M University
300 Olsen Boulevard College Station, TX 77843-2128 (USA)

[c] Dr. F. Wang
California Institute for Biomedical Research (Calibr)
11119 North Torrey Pines Road, La Jolla, CA 92037 (USA)

[d] Dr. M. Convery, Dr. R. Young
Molecular Discovery Research, GSK Medicines Research Centre
Gunnels Wood Road, Stevenage, SG1 2NY (UK)

[e] Dr. D. Calvo, L. Mata
Centro de Investigación Básica
Platform Technologies and Science, GlaxoSmithKline
Parque Tecnológico de Madrid, 28760 Tres Cantos, Madrid (Spain)

Supporting information and the ORCID identification number(s) for the author(s) of this article can be found under <http://dx.doi.org/10.1002/cmdc.201600020>.

isonicotinic acyl radical that has been shown to react with NADH within the InhA active site.^[15] This inhibitory adduct was identified as the acylation product at the 4-position of the nicotinamide moiety of NADH. Resistance to INH, which is one of the hallmarks of MDR strains, has been associated with at least five different genes (*KatG*, *InhA*, *ahpC*, *kasA*, and *ndh*);^[16] although these findings still lack clear biochemical explanations, 60–70% of resistant isolates can be directly linked to defects in the *KatG* gene (often with compensatory mutations in other genes) and less commonly in the *InhA* structural gene and its upstream promoter region.

There has been widespread research^[16–21] into the discovery and development of new inhibitors targeted directly at InhA that do not require prior *KatG* activation, which may result in activity against clinical isolates resistant to INH. With this goal in mind, a high-throughput screening campaign^[22] against InhA was carried out to identify novel direct inhibitors of InhA.

Herein we report the identification of a new series of highly selective direct InhA inhibitors based on the *N*-benzyl-4-((heteroaryl)methyl)benzamide template, including optimization attempts with goals of improving whole-cell activity and the physicochemical profile of the initial hit, as well as an *in vivo* efficacy evaluation of one exemplar in an acute model of TB infection. Additionally, the co-crystal structure of one representative molecule confirming its binding mode within the InhA active site is disclosed.

Results and Discussion

Chemistry

The optimization of validated hit **1** was focused on generating new analogues by modifying four identifiable structural motifs: the right-hand side (RHS: *o*-chloro-*p*-fluorophenyl ring), the left-hand side (LHS: pyrazole), the linker (amide bond), and the central unit (CU: phenyl ring) (Figure 1).

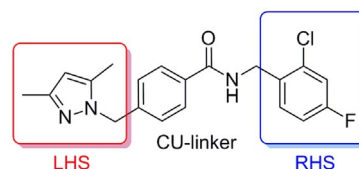
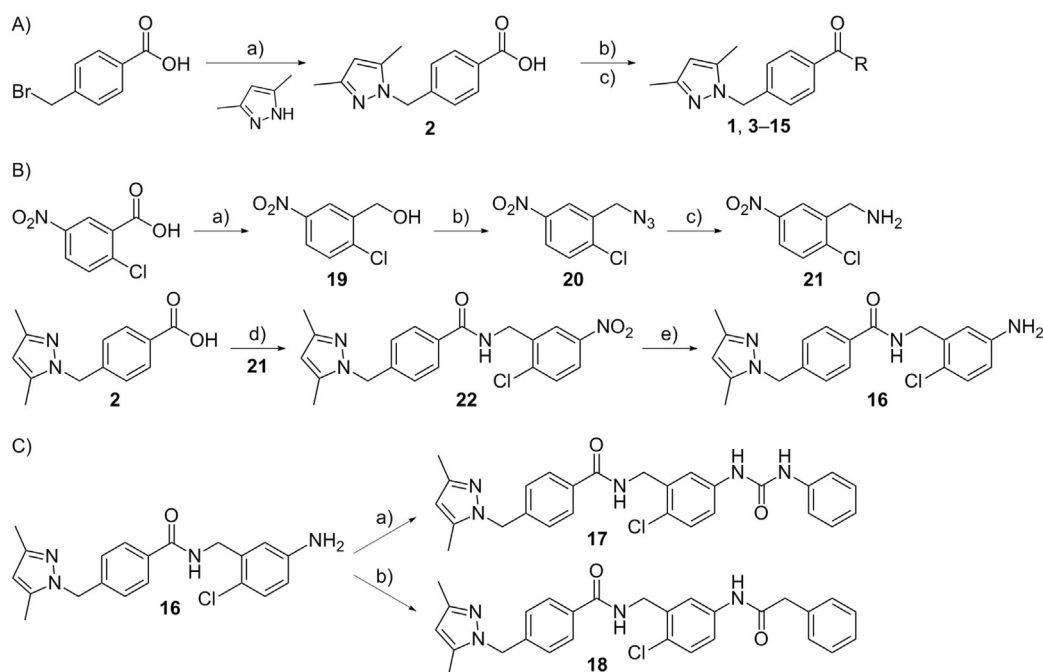


Figure 1. Compound 1: medicinal chemistry optimization priorities.

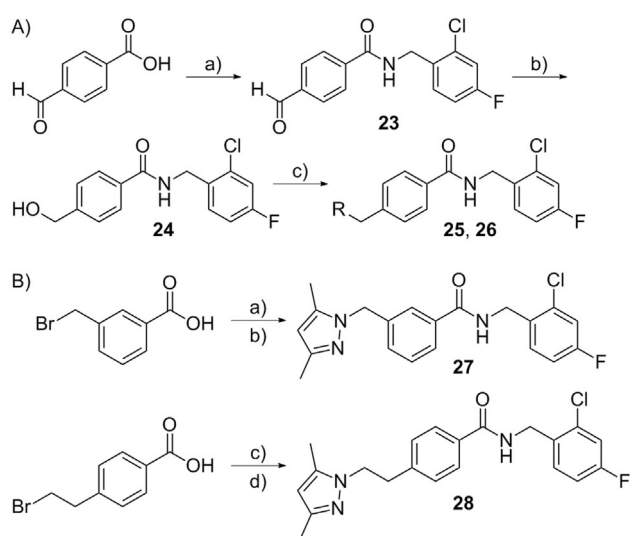
RHS modifications were centered on replacement and/or substitution of the chlorine and fluorine substituents, with variation around position in the ring and also replacement of the phenyl ring by heterocycles (see Table 4 below). Synthesis of these compounds were carried out by amidation reactions using pyrazolymethylbenzoic acid **2** and the desired amine as highlighted in Scheme 1A. Compound **16** (Scheme 1B) offered a convenient starting point to explore extended derivatives



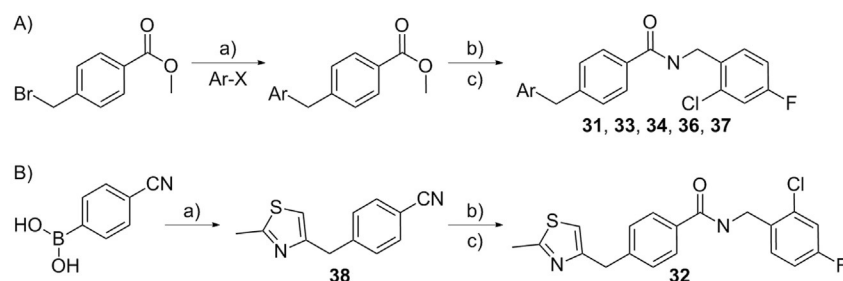
Scheme 1. Compounds listed in Table 4. *Reagents and conditions:* A) a) NaHtBuO (2 equiv), DMF, RT, 30 min, 74%; b) HATU (1.1 equiv), DIPEA (1.5–2 equiv), DMF, RT, 15 min; c) RNH₂ (1–2 equiv), RT, overnight, 50–100%. B) Preparation of compound **16** (Table 4): a) NaBH₄ (4 equiv), BF₃·Et₂O (2.7 equiv), THF, 0 °C, overnight, 90%; b) CBr₄ (1.5 equiv), PPh₃ (1.5 equiv), DMF, RT, 2 h, NaN₃ (3 equiv), overnight, 72%; c) PPh₃ (1.5 equiv), THF/H₂O, RT, overnight, quant.; d) compound **2** (2 equiv), compound **21** (1 equiv), DIPEA (2.5 equiv), EDC (1.2 equiv), DMAP (0.2 equiv), CH₂Cl₂/DMF (10:2), RT, overnight, 29%; e) Fe powder (9 equiv), FeSO₄·7H₂O (2.2 equiv), dioxane/H₂O (5:1), reflux, 6 h, 99%. C) Preparation of compounds **17** and **18** (Table 4): a) isocyanatobenzene (1.1 equiv), CH₂Cl₂, RT, overnight, 44%; b) 2-phenylacetic acid (1.2 equiv), EDCl (1.2 equiv), DMAP (0.2 equiv), DMF, RT, overnight, 5%.

with different substitution or modifications of this amino group, enabling the preparation of a small array based on various coupling reactions. The synthesis of the most potent compounds identified using this approach (**17** and **18**, Table 4) is illustrated in Scheme 1 C.

LHS modifications were centered around two main themes (Figure 2): 1) exploring the spacer and the connecting position between the pyrazole and the phenyl ring (Scheme 2), and 2) replacement of the pyrazole ring with other heterocycles (Scheme 3). Further heterocyclic variation was achieved using Negishi couplings,^[23] starting from commercially available methyl-4-(bromomethyl)benzoate. Hydrolysis of the intermediate ester afforded the corresponding acid, which was subjected to an amidation reaction with 1-(2-chloro-4-fluorophenyl)methanamine to yield the desired products (Scheme 3 A).



Scheme 2. Reagents and conditions: A) Preparation of compounds **25** and **26** (Table 5): a) 1-(2-chloro-4-fluorophenyl)methanamine, HATU, DIPEA, DMF, RT, 3 h, 70%; b) NaBH₄, THF, overnight, 60%; c) (MeSO₂)₂O, DIPEA, DMF followed by azole derivative, polymer-supported BEMP, 10%. B) Preparation of compounds **27** and **28** (Table 5): a) NaOtBu, 3,5-dimethyl-1H-pyrazole, DMF, RT, 2 h, 88%; b) 1-(2-chloro-4-fluorophenyl)methanamine, HATU, DIPEA, DMF, RT, overnight, 43%; c) NaHCO₃, 3,5-dimethyl-1H-pyrazole, MeOH, 135 °C, 2 h, microwave, 26%; d) 1-(2-chloro-4-fluorophenyl)methanamine EDCl, DMAP, DMF, RT, overnight, 35%.



Scheme 3. Reagents and conditions: A) Synthesis of compounds **31**, **33**, **34**, **36**, and **37** (Table 6): a) Zn/THF, reflux, 1.5 h, then Pd(PPh₃)₄, Ar-X, reflux, 3.5 h, 30–40%; b) LiOH, THF/H₂O, RT, overnight, 60–82%; c) 1-(2-chloro-4-fluorophenyl)methanamine, EDCl, DMAP, DMF, RT, overnight, 17–35%. B) Synthesis of compound **32** (Table 6): a) Pd(PPh₃)₄, Na₂CO₃, DME, N₂ atmosphere, 4-(chloromethyl)-2-methyl-1,3-thiazole, 90 °C, overnight, 59%; b) KOH, EtOH/H₂O, overnight, 62%; c) 1-(2-chloro-4-fluorophenyl)methanamine EDCl, DMAP, DMF, RT, overnight, 40%.

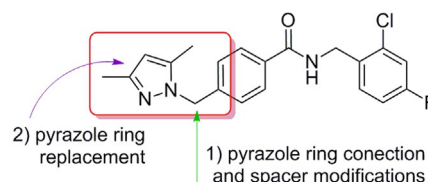


Figure 2. Synthetic scheme for chemical modifications to the LHS.

An exception to this general procedure was the synthesis of compound **32** (Scheme 3 B). In this case the commercial 4-(cyanophenyl)boronic acid was reacted under Suzuki conditions with 4-(chloromethyl)-2-methyl-1,3-thiazole to obtain intermediate **38**. Formation of the corresponding carboxylic acid by nitrile group hydrolysis and ensuing amide formation with 1-(2-chloro-4-fluorophenyl)methanamine afforded the desired compound **32**. Replacement of the pyrazole ring led to the identification of compound **36** (see Table 6 below; preparation in Scheme 3 A), which provided impetus to explore heteroatom variations of the methylene spacer (Figure 3).

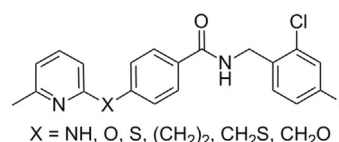
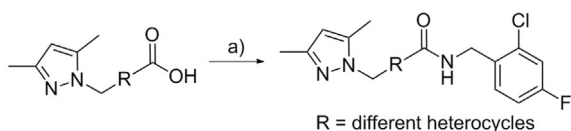


Figure 3. Analogues of compound **36** (compounds **41–46**).

Derivatives listed in Table 7 below (analogues of compound **36**) required a customized synthetic route. Preparative details are provided in the Supporting Information (Schemes 5–10).

Derivatives were also synthesized in order to explore modifications around the central unit (CU) following the general procedure depicted in Scheme 4. The final amide coupling reaction between the corresponding modified acid and 1-(2-chloro-4-fluorophenyl)methanamine afforded the desired compounds **49–51** (Supporting Information). The exception to this general procedure was the synthesis of **48**, which was generated by mesylation of the pyridine-2-carboxamide alcohol analogue to **24** followed by substitution by dimethylpyrazole (Supporting Information).



Scheme 4. General procedure for the synthesis of compounds **49–51** (see Table 10, Supporting Information). *Reagents and conditions:* a) 1-(2-chloro-4-fluorophenyl)methanamine, EDCI, DMAP, DMF, RT, overnight, 10–48%.

To investigate the importance of the amide moiety, various linker modifications were explored. These derivatives (compound **47** in Table 8 below, and compounds **52–57** in Supporting Information Table 11) required specific synthetic pathways which are described in the Supporting Information.

Biology

Amongst the inhibitors identified in the high-throughput screen against InhA,^[22] a number of *N*-benzyl-4-((heteroaryl)methyl)benzamides were highlighted. Compound **1** was identified as a hit of particular interest for further optimization. This compound exhibited good inhibitory potency against InhA ($IC_{50} = 0.05 \mu\text{M}$) in addition to modest antitubercular activity ($MIC_{90} = 10 \mu\text{M}$) without any preliminary evidence of cytotoxicity in the HepG2 assay (Table 1).

The development of a family of *N*-benzamides targeted directly at InhA which do not require prior activation by KatG

Table 1. In vitro biological profile of compound 1.	
InhA IC_{50} [μM] ^[a]	0.05 ± 0.01
<i>M. tuberculosis</i> H ₃₇ Rv MIC_{90} [μM] ^[a]	10
<i>M. bovis</i> InhA overexpressor/WT MIC_{90} ratio	6
Chrom log $D_{7.4}$ ^[b]	5.16
HSA [%] ^[c]	94.63
Solubility CLND [μM] ^[d]	170
CYP 3A4 (VR) pIC_{50}	< 4.3
HepG2 Tox50 [μM]	> 50
clog <i>P</i>	4
Mouse CL_{int} [$\text{mL min}^{-1} \text{g}^{-1}$]	5.7

[a] Values are the mean ± SD of four different assays. [b] pH 7.4. [c] HSA: percent human serum albumin binding with compound. [d] CLND: chemiluminescent nitrogen detection, aqueous solubility.

Table 2. MIC_{90} values [μM] of compounds 1 , 36 , and 47 in H ₃₇ Rv and four clinical <i>M. tuberculosis</i> isolates with KatG mutations in S315T, in comparison with isoniazid (INH) in the same experiments.					
Compd	H ₃₇ Rv	KatG-1	KatG-2	KatG-3	KatG-4
1	10	31	12	12	16
36	31	94	47	47	47
47	31	31	31	23	31
INH	0.5	32	32	23	32

Table 3. MIC_{90} data for compound 1 , kanamycin (KM), isoniazid (INH), and a strain of <i>M. bovis</i> BCG overexpressing InhA.			
Compd	MIC_{90} [μM]		InhA OE/ctrl
	<i>M. bovis</i> BCG pATB45 (ctrl)	<i>M. bovis</i> BCG pATB45– <i>M. tub.</i> InhA (OE)	
1	31	190	6
KM	0.62	0.62	1
INH	1.0	12	12

(Table 2) could lead to a new generation of InhA inhibitors as powerful weapons against MDR-TB^[2–6] and XDR-TB.^[7,8] InhA target engagement was supported by the increased MIC_{90} measured for **1** in the assay of a BCG strain overexpressing InhA (Table 3).

SAR analysis and in vitro properties

The main goal of the medicinal chemistry program was to improve the whole-cell potency of the initial hit, compound **1**, by modifications to the four different regions described above (Figure 1). Furthermore, the optimization process also focused on ligand efficiency metrics ($LE^{[24]}$ and $LLE^{[24]}$) and also on physical properties (clog *P* and property forecast index (PFI)^[25]) in the iterative design of compounds and to help with data analysis (see Figures 7 and 8 and Table 12 in the Supporting Information).

RHS SAR

RHS SAR analysis (Table 4) showed that replacement of the phenyl ring by pyrazole or furan is tolerated (compounds **14** and **15**), although they were not as potent as the parent compound. The result suggests that a phenyl group is better than pyrazole and furan for the RHS. Substituents around the phenyl ring were essential to maintain inhibitory potency (compound **9**), and the best results were observed with *ortho/para* substitution patterns in the aromatic ring, with some tolerance for *meta* substituents. Direct comparison of **1** and **4**, and **3** and **12** with compound **13**, showed the *para/ortho* disubstitution as essential for InhA inhibitory activity.

The observed tolerance of *meta* substitution prompted us to consider compound **16** as a convenient starting point to explore derivatives with different modifications of the amino group. This exercise led to the identification of the most active molecules in terms of both enzymatic and whole-cell activity (**17** and **18**, Table 4). Unfortunately, these improvements came at the cost of high lipophilicity (clog *P* for compounds **17** and **18**: 5.3 and 5.0; LLE : 1.68 and 2.09, respectively), and these two compounds were considered unsuitable for further progression.

LHS SAR

The first set of small LHS modifications around the pyrazole ring resulted in decreased activity (Table 5); direct comparison

Table 4. In vitro activities of select RHS derivatives against *M. tuberculosis* InhA and *M. tuberculosis* H₃₇Rv.

Compd	R	InhA IC ₅₀ [μM] ^[a]	H ₃₇ Rv MIC ₉₀ [μM] ^[c]	Compd	R	InhA IC ₅₀ [μM] ^[a]	H ₃₇ Rv MIC ₉₀ [μM] ^[c]
3		1.00 ± 0.01 ^[b]	ND	12		0.25 ± 0.04	ND
4		1.26 ± 0.03	62	13		3.10 ± 0.06 ^[b]	ND
5		1.58 ± 0.08	125	14		0.12 ± 0.02	31
6		2.51 ± 0.08	62	15		0.09 ± 0.01	46
7		1.58 ± 0.01	62	16		0.35 ± 0.02	94
8		1.58 ± 0.03 ^[b]	62	17		0.09 ± 0.02	6
9		5.93 ± 1.26	> 125	18		0.08 ± 0.01	16
10		2.51 ± 0.04 ^[b]	ND				
11		0.54 ± 0.7	23				

[a] Values are the mean ± SD of four different assays. [b] Values are the mean ± SD of two different assays. [c] ND: not determined.

between compounds **1**, **25**, and **26** showed that a 3-methyl group is essential for activity against the enzyme, as compound **26** was found to be inactive. The additional 5-methyl group was found to be vital to achieving enhanced potency.

In terms of the pyrazole connectivity with the CU, the *para*-benzyl group was favored, whereas the two-carbon homologation was also well tolerated (**27** and **28**). With these data in hand, replacement of the pyrazole motif with other heteroaromatic rings was investigated (Table 6). Methyl monosubstituted 1,3-thiazoles (**31** and **32**) were found to be very potent InhA inhibitors, and a methyl group at the 5-position or no substitution of the ring decreased potency markedly (**33** and **34**).

Replacement of pyrazole motif with isomeric pyridines and other six-membered heterocyclic systems containing two nitrogen atoms was then explored (Table 6). The best pyridine substitution was found to be at position 6, with a methyl group being preferred over a trifluoromethyl substituent (**36** and **37**). Several pyrazines and pyrimidines were also prepared (**58–60**; see Table 9 in the Supporting Information), and were found to be poorly active.

On the basis of the promising profile of compound **36** (IC₅₀: 0.05 μM and *M. tuberculosis* MIC₉₀: 31 μM), the impact of various spacers linking the pyridine ring with the rest of the structure was explored (Figure 3, Table 7). The methylene linker was first replaced by different heteroatoms. Whilst nitrogen- and oxygen-containing structures were found to be inactive (**41** and **42**), the sulfur analogue **43** showed similar levels of InhA inhibition as that of the parent compound **36**. Elongation of the methylene linker into ethyl or methylene-thioether (**45** and **46**) yielded inactive molecules; however, the introduction of oxygen (compound **44**) gave IC₅₀ and MIC₉₀ values similar to those of **36**. Unfortunately, this approach did not lead to an improvement in the whole-cell activity of the initial hit **1**.

Linker and central unit SAR

The replacements with both furan and thiophene resulted in inactive molecules (**48–51**, Table 10 in the Supporting Information), although the pyridine analogue **48** showed moderate enzyme and whole-cell activity. To evaluate the role of the

Table 5. In vitro activities of select pyrazole derivatives against *M. tuberculosis* InhA and *M. tuberculosis* H₃₇Rv: LHS modifications.

Compd	R ¹	R ²	InhA IC ₅₀ [μM] ^[a]	H ₃₇ Rv MIC ₉₀ [μM]
25		H	0.5 ± 0.03 ^[b]	39
26		H	> 10 ^[b]	> 125
27	H		> 10	> 125
28		H	0.32 ± 0.03	62

[a] Values are the mean ± SD of four different assays. [b] Values are the mean ± SD of two different assays.

Table 6. In vitro activities of select pyrazole derivatives against *M. tuberculosis* InhA and *M. tuberculosis* H₃₇Rv: LHS modifications.

Compd	R ¹	InhA IC ₅₀ [μM] ^[a]	H ₃₇ Rv MIC ₉₀ [μM]
31		0.06 ± 0.21 ^[b]	62
32		0.09 ± 0.01	125
33		3.25 ± 0.66	> 125
34		1.40 ± 0.10	> 125
36		0.05 ± 0.01	31
37		0.25 ± 0.05	> 125

[a] Values are the mean ± SD of four different assays. [b] Values are the mean ± SD of two different assays.

amide bond, various linker modifications were explored. The urea (**54**, Supporting Information Table 11) gave modest inhibitory activity against the enzyme. Replacement of the amide by both an ester and a sulfonamide led to a total loss of enzyme inhibition (**52** and **53**, Supporting Information Table 11) and the same outcome was observed if the amide nitrogen was alkylated (**55**, Supporting Information Table 11) or upon removal

Table 7. In vitro activities of select pyrazole derivatives against *M. tuberculosis* InhA and *M. tuberculosis* H₃₇Rv: LHS modifications.

Compd	X	InhA IC ₅₀ [μM] ^[a]	H ₃₇ Rv MIC ₉₀ [μM]
41	NH	> 10	ND
42	O	3.4 ± 0.05	> 125
43	S	0.06 ± 0.01	125
44	CH ₂ O	0.02 ± 0.01	31
45	CH ₂ CH ₂	1.55 ± 0.20	> 125
46	CH ₂ S	0.26 ± 0.04	> 125

[a] Values are the mean ± SD of four different assays; ND: not determined.

of the amide carbonyl group (compound **57**), highlighting the importance of this interaction, which was later rationalized by the crystal structure.

One of the most interesting modifications was the reversed amide **47** (Table 8), which gave enzyme and whole-cell activity at levels similar to those of the initial hit, as well as improved

Table 8. In vitro activities of compound **47** against *M. tuberculosis* InhA and *M. tuberculosis* H₃₇Rv: linker modifications.

Compd	InhA IC ₅₀ [μM]	H ₃₇ Rv MIC ₉₀ [μM]
47	0.04 ± 0.01	31

[a] Values are the mean ± SD of four different assays.

in vitro metabolic stability (CL_{int} = 2.6 mL min⁻¹ g⁻¹). The major shortcomings of compound **1** were the sub-optimal physical attributes, most notably high lipophilicity^[26–28] and relatively modest solubility, so particular efforts were made to investigate analogues with lower lipophilicity (measured as Chrom log *D*_{7.4}^[25] see Figure 8, Supporting Information). This preliminary SAR analysis showed how potency does not appear to be clearly driven by lipophilicity or ligand efficiency (for example, compounds **1**, **15**, **17**, and **18**; Supporting Information Figure 7), and the measured data for many compounds thus gave PFI values (Chrom log *D*_{7.4} + number of aromatic rings) of > 8, a level indicative of poor developability outcomes.

Despite these extensive efforts, no significant overall improvements from compound **1** were achieved; however, this family of compounds did have a reasonable profile in terms of enzyme inhibitory potency and whole-cell activity. Furthermore, exemplars showed InhA target engagement (Supporting Information Table 8) and activity versus KatG mutant clinical isolates (data in Table 2 for compounds **1**, **36**, and **47**).

In vivo properties

The initial hit was progressed to pharmacokinetic (PK) studies (Figure 4, Supporting Information), in which **1** was found to be highly bioavailable (72%) after oral administration in mice, reaching a C_{max} value of $6.5 \mu\text{g mL}^{-1}$ with an encouraging AUC of $39 \mu\text{g h mL}^{-1}$ with sustained exposure. With this information in hand, compound **1** was progressed to efficacy studies in a murine model of acute TB infection, at oral doses of 200 and 500 mg kg^{-1} twice daily (Figure 5, Supporting Information). Unfortunately, no statistically significant decrease in colony-forming units (CFU) counts in the lungs of TB-infected mice was observed relative to untreated controls. The lack of in vivo efficacy for compound **1** could be the result of its modest antitubercular potency which directly impacts the efficacy drivers, AUC/MIC₉₀ and/or C_{max} /AUC.

Structure of the InhA–1 complex

Toward the end of the synthetic program, a ligand crystal structure of the lead compound was solved; this is shown in Figure 4 (PDB ID: 4QXM). In contrast to the previously identified InhA inhibitors such as pyrrolidine carboxamides, Genzyme10850, triclosan, and NITD^[21] compounds, the catalytic residue of Tyr158 did not make any hydrogen bonds with compound **1**, and participated in ligand binding only through van der Waals interactions. This way, the *N*-benzamide template belongs to a new class of compounds recently described in the literature.^[16,29] In addition, in our InhA–NAD⁺–*N*-benzamide structure, the side chain of Phe149 adopted the identical position as observed in the InhA–NAD(H) structure. Unlike the

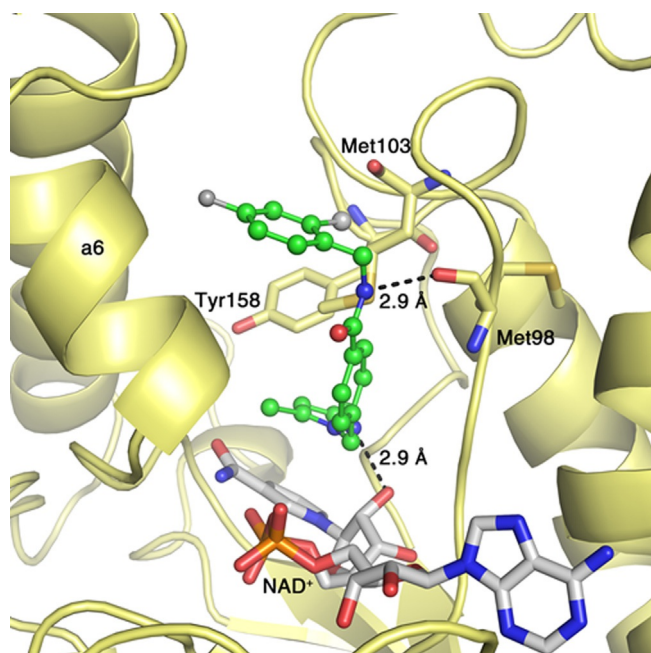


Figure 4. Compound **1** bound to the active site of InhA. Compound **1** is shown in green ball-and-stick format, NAD⁺ in grey as thick lines, and hydrogen bonds as dashed lines. Helix a6, which is ordered in the structure, along with Met98, Met103, and Tyr158 are highlighted.

INH–NADH adduct, our compound did not cause flipping of the Phe149 side chain, and so was not observed to interact with the isonicotinic acid binding pocket.

The crystal structure also revealed that compound **1** is bound to the hydrophobic substrate binding pocket of InhA which is surrounded by residues Met199, Leu207, Ile215, Met103, Phe149, Tyr158, Ala198, and Ile202. The enzyme–inhibitor complex only crystallized in the presence of the NAD(H) cofactor, which indicates the uncompetitive character of the inhibitor.

The direct hydrogen bonding between the carbonyl oxygen atom of the main-chain Met98 and the amide nitrogen atom of the inhibitor (2.9 Å, Figure 4) is the key interaction identified with InhA that provided a rationale for the loss of activity with *N*-methylation (compounds **1** and **55**, Supporting Information Table 11). The carbonyl group of compound **1** is essential for activity (**11** and **57**, Supporting Information Table 11); however, it does not itself establish any hydrogen bonding interactions with the surrounding protein residues. It only shows van der Waals interactions (3.6–3.8 Å) with Ala198 and Phe97.

The main pyrazole ring interactions are with the nicotinamide ring of NAD⁺ via π – π stacking and with the 2'-hydroxy group of the NAD⁺ ribose moiety via hydrogen bonding (2.9 Å). The 3- and 5-methyl groups contribute to compound binding, both being important to maintain potent InhA inhibitory activity. The 3-methyl group makes hydrophobic and van der Waals interactions with the side chains of Phe149 and Tyr158 (3.9 Å) as well as with the nicotinamide ring of NAD⁺, playing an important role in the binding of the compound with the enzyme (comparison of compounds **25** and **26**, Table 5). The presence of the 5-methyl group improves binding with the enzyme (comparison of **1** and **25**, Table 5) making additional van der Waals interactions with Thr196 and NAD⁺ (3.2–3.4 Å).

In the right-hand side of the molecule, the dihalide-substituted phenyl ring interacts with the main-chain Gln100, Met103, Met98, Gly104, Leu207, and Ile202 residues via hydrophobic interactions, with reasonable filling of available space. This is consistent with the improved enzyme activity of compound **1** relative to less heavily substituted analogues **3**, **4**, **9**, and **13**. The presence of a bulkier trifluoromethyl group in **12** at the *ortho* position decreased activity more than one order of magnitude relative to compound **1** (Table 4). This could be due to steric clash with the protein, as the *ortho*-chlorine atom closely packs against Met103 (3 Å).

Conclusions

We have identified a series of *N*-benzyl-4-((heteroaryl)methyl)-benzamides as a novel class of direct InhA inhibitors by high-throughput screening. These compounds demonstrated potent activity against *M. tuberculosis*, maintaining activity versus KatG mutant clinical strains and emerging as a potential tool against MDR-TB and XDR-TB.

Despite the thorough SAR investigation around the hit, no compounds were obtained with significantly improved potency against *M. tuberculosis* H₃₇Rv relative to compound **1**. How-

ever, several derivatives were obtained with similar InhA inhibitory and antibacterial activity (e.g., compounds **11**, **12**, **14**, **15**, **18**, **36**, **44**, and **47**). Compound **1** is a potent direct InhA inhibitor with moderate whole-cell activity and an encouraging safety profile, but unfortunately it was not efficacious in an *in vivo* murine model of TB infection. The SAR information presented for this new antitubercular compound series, rationalized by interactions observed in a co-crystal structure with InhA, should serve as a valuable guide in the design of new molecules toward the goals of improved levels of InhA inhibition and antitubercular whole-cell activity.

Experimental Section

Chemistry

General: All commercially available reagents and solvents were used without further purification unless otherwise stated. High-purity solvents were purchased from commercial vendors and dried with molecular sieves (3–4 Å). Reactions were monitored by thin-layer chromatography (TLC) with silica gel 60 F₂₅₄ plates (thickness 2 mm, Merck); analysis was carried by UV light at λ 254 nm, staining with KMnO₄ and iodine. Reversed-phase liquid chromatography/mass spectrometry (LC–MS) was performed with a Waters 2000 chromatograph equipped with an Agilent 1100 analytical column connected to a high-resolution Micromass ZMD spectrometer. Separation and purification of products was carried out by column chromatography using silica gel (particle size: 30–45 μ m; Isolute). Purifications were performed automatically on a Master-II Flash Biotage instrument. NMR spectroscopy was carried out in the Structural Analysis Department of the Tres Cantos Medicines Development Campus GlaxoSmithKline, using a Varian Unity (300 MHz) and a Bruker DPX (400 MHz). Measurements were made at room temperature and in the deuterated solvent indicated in each case. Chemical shifts (δ) are expressed in parts per million (ppm) using the deuterated solvent as reference (CDCl₃: 7.26 ppm, [D₆]DMSO: 2.49 ppm, CD₃OD: 3.30 ppm); coupling constants (*J*) are expressed in hertz (Hz). NMR signals are abbreviated as follows: s (singlet), d (doublet), t (triplet), q (quartet), qt (quintet), m (multiplet), and br (broad). Mass spectrometry data were collected in the Structural Analysis Department of the Tres Cantos Medicines Development Campus GlaxoSmithKline, using a Waters ZQ2000 instrument coupled with an LC Agilent 1100 or Waters Acquity SQD mass spectrometer. Detailed descriptions of the LC–MS method used with the aforementioned equipment are provided in the Supporting Information.

4-((3,5-dimethyl-1H-pyrazol-1-yl)methyl)benzoic acid (2). In a round-bottom flask, 3,5-dimethylpyrazole (500 mg, 5.2 mmol) was dissolved in DMF (15 mL). Sodium *tert*-butoxide (1 g, 10.4 mmol) was added to this solution, and the mixture was stirred at 25 °C for 15 min. A solution of 4-(bromomethyl)benzoic acid (214 mg, 1 mmol) in DMF (20 mL) was then added dropwise to the initial mixture and stirred for 30 min at 25 °C. The solvent was removed under vacuum, and the residue dissolved in H₂O (200 mL). The solution was acidified to pH 5 with aqueous HCl (2 M), and the resulting precipitate was filtered off to afford the title compound (586 mg, 74%) as a white solid. ¹H NMR (400 MHz, [D₆]DMSO): δ = 12.87 (brs, 1H), 7.88 (d, *J* = 8.0 Hz, 2H), 7.16 (d, *J* = 8.0 Hz, 2H), 5.86 (s, 1H), 5.25 (s, 2H), 2.13 (s, 3H), 2.09 ppm (s, 3H).

N-(2-chloro-4-fluorobenzyl)-4-((3,5-dimethyl-1H-pyrazol-1-yl)methyl)benzamide (1). In a reaction vial compound **2** (50 mg,

0.22 mmol) and HATU (90 mg, 0.25 mmol) were added and dissolved in DMF (15 mL). DIPEA (56 mg, 0.43 mmol) was then added. The mixture was stirred for 10 min. 2-Chloro-4-fluorophenylmethanamine (69 mg, 0.43 mmol) was dissolved in DMF (0.5 mL) and added dropwise to the initial mixture. The reaction was stirred at room temperature for 18 h. The solvent was removed under vacuum. The resulting residue was dissolved in CH₂Cl₂ (2 mL) and washed with saturated NaHCO₃ (2 mL). The organic layer was dried over MgSO₄, and volatiles were removed under vacuum. The resulting crude was purified by column chromatography to yield 56.5 mg of the title compound as a white solid (70%). ¹H NMR (400 MHz, [D₆]DMSO): δ = 9.01 (t, *J* = 5.8 Hz, 1H), 7.86 (d, *J* = 8.1 Hz, 2H), 7.42 (dd, *J* = 2.7, 8.7 Hz, 1H), 7.38 (dd, *J* = 6.3, 8.6 Hz, 1H), 7.22–7.13 (m, 3H), 5.88 (s, 1H), 5.26 (s, 2H), 4.49 (d, *J* = 5.8 Hz, 2H), 2.15 (s, 3H), 2.10 ppm (s, 3H); ¹³C NMR (101 MHz, [D₆]DMSO): δ = 166.1, 160.9 (d, *J* = 245.9 Hz, 1C), 146.2, 141.2, 139.2, 133.1, 132.7 (d, *J* = 3.7 Hz, 1C), 132.6 (d, *J* = 11.0 Hz, 1C), 130.1 (d, *J* = 9.5 Hz, 1C), 127.6 (s, 2C), 126.8 (s, 2C), 116.4 (d, *J* = 24.9 Hz, 1C), 114.2 (d, *J* = 21.2 Hz, 1C), 105.2, 51.2, 40.1, 13.2, 10.6 ppm; LC–MS: *t*_R = 1.21 min, *m/z* 371.12 [M + H]⁺; purity: > 95%.

N-(2-trifluorobenzyl)-4-((3,5-dimethyl-1H-pyrazol-1-yl)methyl)benzamide (3). 2-Trifluorophenylmethanamine (47 mg, 0.43 mmol) and carboxylic acid **2** (50 mg, 0.22 mmol) were mixed following the procedure described for **1** to yield 72 mg of the title compound as a white oil (86%). ¹H NMR (400 MHz, [D₆]DMSO): δ = 9.07 (t, *J* = 5.8 Hz, 1H), 7.87 (d, *J* = 8.1 Hz, 2H), 7.72 (d, *J* = 7.6 Hz, 1H), 7.67–7.58 (m, 1H), 7.53–7.39 (m, 2H), 7.18 (d, *J* = 8.1 Hz, 2H), 5.88 (s, 1H), 5.26 (s, 2H), 4.64 (d, *J* = 5.6 Hz, 2H), 2.16 (s, 3H), 2.10 ppm (s, 3H); ¹³C NMR (101 MHz, [D₆]DMSO): δ = 166.2, 146.2, 141.3, 139, 137.6, 133, 132.6, 128.1, 127.6 (s, 2C), 127.3, 126.8 (s, 2C), 126.2, 125.8, 125.7 (d, *J* = 5.9 Hz, 1C), 105.2, 51.2, 39.2, 13.3, 10.6 ppm; LC–MS: *t*_R = 1.22 min, *m/z* 387.16 [M + H]⁺; purity: > 95%.

N-(2-chlorobenzyl)-4-((3,5-dimethyl-1H-pyrazol-1-yl)methyl)benzamide (4). 2-Chlorophenylmethanamine (61.5 mg, 0.43 mmol) and carboxylic acid **2** (50 mg, 0.22 mmol) were mixed following the procedure described for **1** to yield 56 mg of the title compound as a colorless oil (73%). ¹H NMR (400 MHz, [D₆]DMSO): δ = 9.00 (t, *J* = 5.8 Hz, 1H), 7.85 (d, *J* = 8.3 Hz, 2H), 7.46–7.40 (m, 1H), 7.34–7.25 (m, 3H), 7.17 (d, *J* = 8.1 Hz, 2H), 5.87 (s, 1H), 5.25 (s, 2H), 4.52 (d, *J* = 5.8 Hz, 2H), 2.15 (s, 3H), 2.09 ppm (s, 3H); ¹³C NMR (101 MHz, [D₆]DMSO): δ = 166.1, 146.2, 141.2, 139, 136.3, 133.1, 131.9, 129.1, 128.5, 128.5, 127.6 (s, 2C), 127.1, 126.7 (s, 2C), 105.1, 51.2, 40.5, 13.3, 10.6 ppm; LC–MS: *t*_R = 1.20 min, *m/z* 353.13 [M + H]⁺; purity: > 95%.

N-(3-propan-2-yloxybenzyl)-4-((3,5-dimethyl-1H-pyrazol-1-yl)methyl)benzamide (5). 3-Propan-2-yloxyphenylmethanamine (71.7 mg, 0.43 mmol) and carboxylic acid **2** (50 mg, 0.22 mmol) were mixed following the procedure described for **1** to yield 58.5 mg of the title compound as a white solid (71%). ¹H NMR (400 MHz, [D₆]DMSO): δ = 8.95 (t, *J* = 5.9 Hz, 1H), 7.83 (d, *J* = 8.3 Hz, 2H), 7.23–7.16 (m, 1H), 7.15 (d, *J* = 8.1 Hz, 2H), 6.84–6.79 (m, 2H), 6.78–6.73 (m, 1H), 5.87 (s, 1H), 5.24 (s, 2H), 4.55 (t, *J* = 6.0 Hz, 1H), 4.41 (d, *J* = 6.1 Hz, 2H), 2.14 (s, 3H), 2.10 (s, 3H), 1.23 (s, 3H), 1.22 ppm (s, 3H); ¹³C NMR (101 MHz, [D₆]DMSO): δ = 165.9, 157.4, 146.2, 141.3, 141, 139, 133.3, 129.3, 127.5 (s, 2C), 126.7 (s, 2C), 119, 114.5, 113.5, 105.2, 68.9, 51.2, 42.5, 21.8 (s, 2C), 13.3, 10.6 ppm; LC–MS: *t*_R = 1.22 min, *m/z* 377.21 [M + H]⁺; purity: > 95%.

N-(2-nitrobenzyl)-4-((3,5-dimethyl-1H-pyrazol-1-yl)methyl)benzamide (6). 2-Nitrophenylmethanamine (66.5 mg, 0.43 mmol) and carboxylic acid **2** (50 mg, 0.22 mmol) were mixed following the procedure described for **1** to yield 61.6 mg of the title compound

as a brown solid (65%). $^1\text{H NMR}$ (400 MHz, $[\text{D}_6]\text{DMSO}$): δ = 9.07 (t, J = 5.7 Hz, 1H), 8.02 (dd, J = 1.0, 8.1 Hz, 1H), 7.83 (d, J = 8.3 Hz, 2H), 7.70 (dt, J = 1.1, 7.6 Hz, 1H), 7.57–7.47 (m, 2H), 7.17 (d, J = 8.3 Hz, 2H), 5.87 (s, 1H), 5.25 (s, 2H), 4.73 (d, J = 5.8 Hz, 2H), 2.15 (s, 3H), 2.10 ppm (s, 3H); $^{13}\text{C NMR}$ (101 MHz, $[\text{D}_6]\text{DMSO}$): δ = 166, 148, 146.2, 141.3, 139, 134.2, 133.7, 132.9, 129.2, 128.2, 127.6 (s, 2C), 126.8 (s, 2C), 124.5, 105.2, 51.2, 39.9, 13.3, 10.6 ppm; LC–MS: t_{R} = 1.14 min, m/z 364.15 $[\text{M} + \text{H}]^+$; purity: > 95%.

***N*-(3-bromobenzyl)-4-((3,5-dimethyl-1H-pyrazol-1-yl)methyl)benzamide (7).** 3-Bromophenylmethanamine (80 mg, 0.43 mmol) and carboxylic acid **2** (100 mg, 0.43 mmol) were mixed following the procedure described for **1** to yield 143 mg of the title compound as a colorless oil (84%). $^1\text{H NMR}$ (400 MHz, $[\text{D}_6]\text{DMSO}$): δ = 9.03 (t, J = 5.9 Hz, 1H), 7.82 (d, J = 8.3 Hz, 2H), 7.48 (s, 1H), 7.43 (td, J = 1.8, 7.0 Hz, 1H), 7.32–7.25 (m, 2H), 7.15 (d, J = 8.1 Hz, 2H), 5.86 (s, 1H), 5.24 (s, 2H), 4.45 (d, J = 5.8 Hz, 2H), 2.14 (s, 3H), 2.09 ppm (s, 3H); $^{13}\text{C NMR}$ (101 MHz, $[\text{D}_6]\text{DMSO}$): δ = 165.9, 146.2, 142.5, 141.3, 138.9, 133.1, 130.5, 129.9, 129.6, 127.5 (s, 2C), 126.7 (s, 2C), 126.2, 121.5, 105.1, 51.2, 42, 13.3, 10.6 ppm; LC–MS: t_{R} = 1.22 min, m/z 397.08 $[\text{M} + \text{H}]^+$; purity: > 95%.

***N*-(3-chlorobenzyl)-4-((3,5-dimethyl-1H-pyrazol-1-yl)methyl)benzamide (8).** 3-Chlorophenylmethanamine (61.5 mg, 0.434 mmol) and carboxylic acid **2** (50 mg, 0.22 mmol) were mixed following the procedure described for **1** to yield 47.4 mg of the title compound as a yellow solid (62%). $^1\text{H NMR}$ (400 MHz, $[\text{D}_6]\text{DMSO}$): δ = 9.03 (t, J = 5.9 Hz, 1H), 7.83 (d, J = 8.1 Hz, 2H), 7.38–7.23 (m, 4H), 7.16 (d, J = 8.3 Hz, 2H), 5.87 (s, 1H), 5.24 (s, 2H), 4.45 (d, J = 5.8 Hz, 2H), 2.14 (s, 3H), 2.09 ppm (s, 3H); $^{13}\text{C NMR}$ (101 MHz, $[\text{D}_6]\text{DMSO}$): δ = 166, 146.2, 142.3, 141.2, 139, 133.1, 132.9, 130.2, 127.5 (s, 2C), 127, 126.7 (s, 2C), 126.7, 125.8, 105.1, 51.2, 42.1, 13.3, 10.6 ppm; LC–MS: t_{R} = 1.19 min, m/z 353.13 $[\text{M} + \text{H}]^+$; purity: > 95%.

***N*-(benzyl)-4-((3,5-dimethyl-1H-pyrazol-1-yl)methyl)benzamide (9).** Phenylmethanamine (0.025 mL, 0.23 mmol) and carboxylic acid **2** (53.7 mg, 0.23 mmol) were mixed following the procedure described for **1** to yield 110 mg of the title compound as a white solid (100%). $^1\text{H NMR}$ (400 MHz, $[\text{D}_6]\text{DMSO}$): δ = 8.99 (t, J = 5.9 Hz, 1H), 7.83 (d, J = 8.3 Hz, 2H), 7.34–7.26 (m, 4H), 7.23 (td, J = 2.9, 6.1 Hz, 1H), 7.15 (d, J = 8.1 Hz, 2H), 5.86 (s, 1H), 5.24 (s, 2H), 4.46 (d, J = 5.8 Hz, 2H), 2.14 (s, 3H), 2.09 ppm (s, 3H); $^{13}\text{C NMR}$ (101 MHz, $[\text{D}_6]\text{DMSO}$): δ = 165.9, 146.2, 141.1, 139.6, 139, 133.3, 128.2 (s, 2C), 127.5 (s, 2C), 127.1, 126.7 (s, 3C), 105.1, 51.2, 42.5, 13.3, 10.6 ppm; LC–MS: t_{R} = 1.15 min, m/z 319.17 $[\text{M} + \text{H}]^+$; purity: > 95%.

***N*-(3-methanesulfonybenzyl)-4-((3,5-dimethyl-1H-pyrazol-1-yl)methyl)benzamide (10).** 3-Methanesulfonylphenylmethanamine (60.4 mg, 0.434 mmol) and carboxylic acid **2** (50 mg, 0.22 mmol) were mixed following the procedure described for **1** to yield 47.9 mg of the title compound as a white solid (55%). $^1\text{H NMR}$ (400 MHz, $[\text{D}_6]\text{DMSO}$): δ = 9.12 (t, J = 5.9 Hz, 1H), 7.87–7.77 (m, 4H), 7.65 (d, J = 7.8 Hz, 1H), 7.60 (t, J = 7.6 Hz, 1H), 7.17 (d, J = 8.1 Hz, 2H), 5.89 (s, 1H), 5.26 (s, 2H), 4.56 (d, J = 5.8 Hz, 2H), 3.18 (s, 3H), 2.15 (s, 3H), 2.10 ppm (s, 3H); $^{13}\text{C NMR}$ (101 MHz, $[\text{D}_6]\text{DMSO}$): δ = 166.1, 146.2, 141.3, 141.1, 140.9, 139.2, 133.1, 132.3, 129.5, 127.6 (s, 2C), 126.8 (s, 2C), 125.4, 125.4, 105.3, 51.2, 43.5, 42.3, 13.2, 10.6 ppm; LC–MS: t_{R} = 1.04 min, m/z 397.15 $[\text{M} + \text{H}]^+$; purity: > 95%.

***N*-(3-chlorobenzyl)-4-((3,5-dimethyl-1H-pyrazol-1-yl)methyl)benzamide (11).** 3-Chlorophenylmethanamine (80 mg, 0.434 mmol) and carboxylic acid **2** (100 mg, 0.43 mmol) were mixed following the procedure described for **1** to yield 140 mg of the title compound as a white solid (82%). $^1\text{H NMR}$ (400 MHz, $[\text{D}_6]\text{DMSO}$): δ =

9.01 (t, J = 5.7 Hz, 1H), 7.86 (d, J = 8.3 Hz, 2H), 7.64–7.58 (m, 1H), 7.37–7.32 (m, 1H), 7.31–7.27 (m, 1H), 7.25–7.18 (m, 1H), 7.17 (d, J = 8.3 Hz, 2H), 5.86 (s, 1H), 5.24 (s, 2H), 4.48 (d, J = 5.8 Hz, 2H), 2.15 (s, 3H), 2.09 ppm (s, 3H); $^{13}\text{C NMR}$ (101 MHz, $[\text{D}_6]\text{DMSO}$): δ = 166.1, 146.2, 141.3, 138.9, 137.8, 133.1, 132.3, 128.9, 128.5, 127.7, 127.6 (s, 2C), 126.7 (s, 2C), 122.2, 105.1, 51.2, 43, 13.3, 10.6 ppm; LC–MS: t_{R} = 1.21 min, m/z 397.08 $[\text{M} + \text{H}]^+$; purity: > 95%.

***N*-(4-fluoro-2-(trifluoromethyl)benzyl)-4-((3,5-dimethyl-1H-pyrazol-1-yl)methyl)benzamide (12).** 4-Fluoro-2-(trifluoromethyl)phenylmethanamine (63.5 mg, 0.434 mmol) and carboxylic acid **2** (50 mg, 0.22 mmol) were mixed following the procedure described for **1** to yield 51.5 mg of the title compound as a white solid (70%). $^1\text{H NMR}$ (400 MHz, $[\text{D}_6]\text{DMSO}$): δ = 9.07 (t, J = 5.8 Hz, 1H), 7.85 (d, J = 8.3 Hz, 2H), 7.62 (dd, J = 2.5, 9.1 Hz, 1H), 7.57–7.47 (m, 2H), 7.17 (d, J = 8.1 Hz, 2H), 5.87 (s, 1H), 5.25 (s, 2H), 4.60 (d, J = 5.6 Hz, 2H), 2.15 (s, 3H), 2.09 ppm (s, 3H); $^{13}\text{C NMR}$ (101 MHz, $[\text{D}_6]\text{DMSO}$): δ = 166.2, 160.5 (d, J = 244.4 Hz, 1C), 146.2, 141.4, 138.9, 133.8 (q, J = 1.5 Hz, 1C), 132.9, 130.9 (d, J = 8.1 Hz, 1C), 127.6 (s, 2C), 128 (qt, J = 31.5 Hz, 1C), 126.7 (s, 2C), 125.1 (dq, J = 2.9, 274.4 Hz, 1C), 119.4 (d, J = 21.2 Hz, 1C), 113.4 (dd, J = 5.9, 25.6 Hz, 1C), 105.1, 51.2, 38.9, 13.3, 10.6 ppm; LC–MS: t_{R} = 1.24 min, m/z 405.15 $[\text{M} + \text{H}]^+$; purity: > 95%.

***N*-(4-fluorobenzyl)-4-((3,5-dimethyl-1H-pyrazol-1-yl)methyl)benzamide (13).** 4-Fluorophenylmethanamine (64.5 mg, 0.434 mmol) and carboxylic acid **2** (50 mg, 0.22 mmol) were mixed following the procedure described for **1** to yield 75.5 mg of the title compound as a yellow solid (100%). $^1\text{H NMR}$ (400 MHz, $[\text{D}_6]\text{DMSO}$): δ = 9.00 (t, J = 5.9 Hz, 1H), 7.82 (d, J = 8.1 Hz, 2H), 7.33 (dd, J = 5.8, 8.6 Hz, 2H), 7.18–7.09 (m, 4H), 5.87 (s, 1H), 5.24 (s, 2H), 4.43 (d, J = 5.8 Hz, 2H), 2.14 (s, 3H), 2.09 ppm (s, 3H); $^{13}\text{C NMR}$ (101 MHz, $[\text{D}_6]\text{DMSO}$): δ = 165.9, 160.9 (d, J = 241.5 Hz, 1C), 146.2, 141, 139, 135.8 (d, J = 2.9 Hz, 1C), 133.3, 129.1 (d, J = 8.1 Hz, 2C), 127.5 (s, 2C), 126.7 (s, 2C), 115 (d, J = 21.2 Hz, 2C), 105.2, 51.2, 41.9, 13.3, 10.6 ppm; LC–MS: t_{R} = 1.15 min, m/z 337.39 $[\text{M} + \text{H}]^+$; purity: > 95%.

***N*-(4-fluorobenzyl)-4-((2-methyl-5-trifluoromethyl)furan-3-yl)methyl)benzamide (14).** (5-Methyl-2-(trifluoromethyl)furan-3-yl)methanamine (38.9 mg, 0.21 mmol) and compound **2** (50 mg, 0.21 mmol) were mixed following the procedure described for **1** to yield 50 mg of the title compound as a white solid (59%). $^1\text{H NMR}$ (400 MHz, $[\text{D}_6]\text{DMSO}$): δ = 8.94 (t, J = 5.8 Hz, 1H), 7.80 (d, J = 8.1 Hz, 2H), 7.15 (d, J = 8.3 Hz, 2H), 6.25 (s, 1H), 5.85 (s, 1H), 5.23 (s, 2H), 4.36 (d, J = 4.5 Hz, 2H), 2.27 (s, 3H), 2.13 (s, 3H), 2.09 ppm (s, 3H); $^{13}\text{C NMR}$ (101 MHz, $[\text{D}_6]\text{DMSO}$): δ = 166, 154.8, 146.2, 141.3, 138.8, 133–132.9 (m, 1C), 133.4–132.7 (m, 1C), 127.9 (d, J = 2.2 Hz, 1C), 127.5 (s, 2C), 126.7 (s, 2C), 121.3–118.5 (m, 1C), 108.9, 105.1, 51.2, 33, 13.3, 13, 10.6 ppm; LC–MS: t_{R} = 1.24 min, m/z 391.15 $[\text{M} + \text{H}]^+$; purity: > 95%.

***N*-(4-bromo-1-ethyl-1H-pyrazol-5-yl)methyl)-4-((3,5-dimethyl-1H-pyrazol-1-yl)methyl)benzamide (15).** (4-Bromo-1-ethyl-1H-pyrazol-5-yl)methylamine (44.3 mg, 0.21 mmol) and carboxylic acid **2** (50 mg, 0.21 mmol) were mixed following the procedure described for **1** to yield 45 mg of the title compound as a white solid (50%). $^1\text{H NMR}$ (400 MHz, $[\text{D}_6]\text{DMSO}$): δ = 8.91 (t, J = 5.2 Hz, 1H), 7.83–7.74 (m, J = 8.3 Hz, 2H), 7.51 (s, 1H), 7.17–7.09 (m, J = 8.3 Hz, 2H), 5.84 (s, 1H), 5.22 (s, 2H), 4.51 (d, J = 5.3 Hz, 2H), 4.17 (q, J = 7.3 Hz, 2H), 2.13 (s, 3H), 2.08 (s, 3H), 1.26 ppm (t, J = 7.2 Hz, 3H); $^{13}\text{C NMR}$ (101 MHz, $[\text{D}_6]\text{DMSO}$): δ = 166, 146.2, 141.3, 138.9, 138, 136.6, 132.8, 127.6 (s, 2C), 126.7 (s, 2C), 105.1, 93.2, 51.2, 44.9, 32.5, 15.3, 13.3, 10.6 ppm; LC–MS: t_{R} = 1.13 min, m/z 415.10 $[\text{M} + \text{H}]^+$; purity: > 95%.

(2-chloro-5-nitrophenyl)methanol (19). 2-Chloro-5-nitrobenzoic acid (3 g, 14.9 mmol) was added to a stirred suspension of NaBH₄ (2.2 g, 59.4 mmol) in dry THF (80 mL) at 0 °C. Then boron trifluoride etherate (5 mL, 40 mmol) was slowly incorporated, leaving the reaction mixture to reach room temperature overnight. The solvent was removed under vacuum, and the resulting crude was dissolved in CH₂Cl₂ and washed with HCl (1 N) and brine. The organic layer was dried over MgSO₄, filtered off, and volatiles were evaporated under vacuum. The residue was purified by column chromatography to yield 2.5 g of the title compound as a white solid (90%). ¹H NMR (300 MHz, CDCl₃): δ = 8.46 (d, *J* = 2.6 Hz, 1H), 8.10 (dd, *J* = 2.3, 8.6 Hz, 1H), 7.52 (d, *J* = 8.8 Hz, 1H), 4.87 (d, *J* = 4.1 Hz, 2H), 2.10 ppm (brs, 1H).

2-(azidomethyl)-1-chloro-4-nitrobenzene (20). Triphenylphosphine (5.9 g, 19.5 mmol) followed by CBr₄ (6.4 g, 19.5 mmol) were added to a stirred solution of alcohol **19** (2.4 g, 13 mmol) in DMF (60 mL) at 0 °C, and the mixture was left stirring for 2 h, reaching room temperature. NaN₃ (2.53 g, 39 mmol) was then incorporated in several portions, and the reaction was left stirring overnight. The solvent was removed under vacuum, and the resulting crude was dissolved in *t*BuOMe and washed with NaHCO₃ (10%) and brine. The organic layer was dried over MgSO₄, filtered off, and the volatiles were evaporated under vacuum. The residue was purified by column chromatography to yield 2 g of the title compound as a colorless oil (72%). ¹H NMR (300 MHz, CDCl₃): δ = 8.33 (d, *J* = 2.6 Hz, 1H), 8.16 (dd, *J* = 2.4, 8.7 Hz, 1H), 7.59 (d, *J* = 8.8 Hz, 1H), 4.62 ppm (s, 2H).

***N*-(2-chloro-5-nitrobenzyl)-4-((3,5-dimethyl-1*H*-pyrazol-1-yl)methyl)benzamide (22).** (2-Chloro-5-nitrophenyl)methanamine (21·H₂O; 0.33 mL, 18 mmol) was added to a stirred solution of azide derivative **20** (1.95 g, 9.2 mmol) and triphenylphosphine (3.6 g, 13.7 mmol) in THF (50 mL) at room temperature. The mixture was left under stirring overnight. The solvent was removed under vacuum, and the resulting crude was dissolved in *t*BuOMe and washed with HCl (4 N). The resulting precipitate was filtered and washed with *t*BuOMe to yield 0.5 g of the title compound as a brown hydrochloride salt (quant). A solution of benzyl amine **21** (1 g, 4.3 mmol) in CH₂Cl₂ (2 mL) was added to a mixture of carboxylic acid **2** (0.5 g, 2.17 mmol), EDCI (0.5 g, 2.6 mmol), and DIPEA (0.72 mL, 4.5 mmol) in CH₂Cl₂/DMF (10 mL/2 mL). Then DMAP was added in one portion, and the mixture was stirred at room temperature overnight. The solvent was removed under vacuum. The resulting residue was dissolved in EtOAc and washed with H₂O. The organic layer was dried over MgSO₄, and the volatiles were removed under vacuum. The resulting crude was purified by column chromatography to yield 300 mg of the title compound (29%). ¹H NMR (300 MHz, CDCl₃): δ = 8.28 (d, *J* = 2.6 Hz, 1H), 8.09 (dd, *J* = 2.5, 8.5 Hz, 1H), 7.75 (d, *J* = 8.1 Hz, 2H), 7.55 (d, *J* = 8.8 Hz, 1H), 7.11 (d, *J* = 7.9 Hz, 2H), 6.83 (brs, 1H), 5.86 (s, 1H), 5.24 (s, 2H), 4.76 (d, *J* = 6.2 Hz, 2H), 2.24 (s, 3H), 2.14 ppm (s, 3H).

***N*-(2-chloro-5-aminobenzyl)-4-((3,5-dimethyl-1*H*-pyrazol-1-yl)methyl)benzamide (16).** A solution of nitro derivative **22** (0.25 g, 0.62 mmol) in dioxane/H₂O (5 mL/1 mL) was treated with iron powder (0.32 g, 5.6 mmol) and FeSO₄·7H₂O (0.38 g, 1.4 mmol) and stirred at reflux for 6 h. It was then cooled to room temperature and filtered through Celite. The filtrate was eluted with EtOAc and washed with NaHCO₃ (10%). The organic layer was dried over MgSO₄, and the volatiles were removed under vacuum to yield 230 mg of the title compound as a yellow solid (99%). ¹H NMR (300 MHz, CDCl₃): δ = 7.71 (d, *J* = 8.1 Hz, 2H), 7.17–7.05 (m, 3H), 6.76 (d, *J* = 2.6 Hz, 1H), 6.65–6.42 (m, 2H), 5.86 (s, 1H), 5.24 (s, 2H), 4.60 (d, *J* = 6.0 Hz, 2H), 3.65 (brs, 2H), 2.27–2.19 (m, 3H), 2.17–

2.08 ppm (m, 3H); LC–MS: *t*_R = 2.47 min, *m/z* 368.14 [*M* + *H*]⁺; purity: > 95%.

***N*-(2-chloro-5-(3-phenylureido)benzyl)-4-((3,5-dimethyl-1*H*-pyrazol-1-yl)methyl)benzamide (17).** A mixture of aniline **16** (50 mg, 0.13 mmol) and phenyl isocyanate (17 mg, 0.14 mmol) in CH₂Cl₂ (5 mL) was left under stirring at 25 °C overnight. The white precipitate was filtered off and washed with CH₂Cl₂ to afford 28 mg of the title compound as a white solid (44%). ¹H NMR (400 MHz, [D₆]DMSO): δ = 9.03 (t, *J* = 5.8 Hz, 1H), 8.78 (s, 1H), 8.53 (s, 1H), 7.89 (d, *J* = 8.3 Hz, 2H), 7.55 (dd, *J* = 2.5, 8.6 Hz, 1H), 7.38 (d, *J* = 7.6 Hz, 2H), 7.33 (d, *J* = 8.6 Hz, 1H), 7.28–7.21 (m, 3H), 7.18 (d, *J* = 8.1 Hz, 2H), 6.95 (t, *J* = 7.3 Hz, 1H), 5.86 (s, 1H), 5.25 (s, 2H), 4.48 (d, *J* = 5.8 Hz, 2H), 2.16 (s, 3H), 2.09 ppm (s, 3H); ¹³C NMR (101 MHz, [D₆]DMSO): δ = 166.1, 152.3, 146.2, 141.4, 139.5, 138.9, 138.9, 136.6, 133.1, 129.3, 128.7 (s, 2C), 127.6 (s, 2C), 126.8 (s, 2C), 124, 121.9, 118.2 (s, 2C), 117.8, 117.5, 105.1, 51.2, 40.4, 13.3, 10.6 ppm; LC–MS: *t*_R = 2.72 min, *m/z* 487.18 [*M* + *H*]⁺; purity: > 95%.

***N*-(2-chloro-5-(2-phenylacetamido)benzyl)-4-((3,5-dimethyl-1*H*-pyrazol-1-yl)methyl)benzamide (18).** A mixture of aniline **16** (50 mg, 0.13 mmol) and phenylacetic acid (22 mg, 0.16 mmol) was treated following the procedure described for benzamide **22**. The purification in this case was performed by preparative HPLC to yield 3 mg of the title compound as a white solid (4.7%). ¹H NMR (300 MHz, CD₃OD): δ = 7.85 (d, *J* = 8.3 Hz, 2H), 7.66–7.48 (m, 2H), 7.42–7.20 (m, 6H), 7.16 (d, *J* = 8.3 Hz, 2H), 6.00 (s, 1H), 5.33 (s, 2H), 4.61 (s, 3H), 3.61 (s, 2H), 2.22 ppm (d, *J* = 3.4 Hz, 6H); LC–MS: *t*_R = 2.73 min, *m/z* 486.18 [*M* + *H*]⁺; purity: > 95%.

***N*-[(2-chloro-4-fluorophenyl)methyl]-4-formylbenzamide (23).** 4-Carboxybenzaldehyde (3 g, 19.9 mmol) and 2-chloro-4-fluorophenylmethanamine (3.4 g, 19.9 mmol) was added following the procedure described for compound **1** to yield 5.8 g of the title compound (100%). ¹H NMR (400 MHz, [D₆]DMSO): δ = 10.08 (s, 1H), 9.26 (t, *J* = 5.5 Hz, 1H), 8.12–8.05 (m, 2H), 8.04–7.98 (m, 2H), 7.51–7.35 (m, 2H), 7.21 (dt, *J* = 2.5, 8.5 Hz, 1H), 4.52 ppm (d, *J* = 5.5 Hz, 2H).

***N*-[(2-chloro-4-fluorophenyl)methyl]-4-(hydroxymethyl)benzamide (24).** Aldehyde **23** (5.8 g, 19.9 mmol) was added to a stirred suspension of NaBH₄ (1.15 g, 30.4 mmol) in dry THF (30 mL) at 0 °C. The mixture was left to reach room temperature for 2 h. MeOH was then added dropwise (20 mL), and the reaction was kept under stirring for 20 min. The solvent was removed under vacuum, and the resulting crude was dissolved in EtOAc and washed with H₂O and brine. The organic layer was dried over MgSO₄, filtered off, and the volatiles were evaporated under vacuum to yield 3.5 g of the title compound as a pale-yellow solid (58%). ¹H NMR (400 MHz, [D₆]DMSO): δ = 8.99 (t, *J* = 5.8 Hz, 1H), 7.86 (d, *J* = 8.5 Hz, 2H), 7.44 (dd, *J* = 2.8, 8.8 Hz, 1H), 7.40 (d, *J* = 8.5 Hz, 2H), 7.39–7.36 (m, *J* = 6.5 Hz, 1H), 7.20 (dt, *J* = 3.0, 8.5 Hz, 1H), 5.30 (t, *J* = 5.5 Hz, 1H), 4.55 (d, *J* = 5.5 Hz, 2H), 4.49 ppm (d, *J* = 5.5 Hz, 2H).

***N*-[(2-chloro-4-fluorophenyl)methyl]-4-[(3-methyl-1*H*-pyrazol-1-yl)methyl]benzamide (25).** Compound **24** (60 mg, 0.2 mmol) was dissolved in anhydrous THF at room temperature. Then methanesulfonic anhydride (42 mg, 0.25 mmol) and DIPEA (0.052 mL, 0.3 mmol) were added, and the mixture was stirred for 30 min. A solution of 3-methyl-1*H*-pyrazole (32.8 mg, 0.4 mmol) and polymer-supported BEMP (82.2 mg, 0.3 mmol) in CH₂Cl₂ was then added to the initial mixture, and the reaction was held at reflux (60 °C) for 48 h. The polymer-supported BEMP was then filtered out, and the solvent was removed under vacuum. The resulting crude was then purified by preparative HPLC to yield 10 mg of the title compound (10%). ¹H NMR (400 MHz, CDCl₃): δ = 7.72 (d, *J* = 8.3 Hz, 2H), 7.43

(dd, $J=6.1, 8.6$ Hz, 1H), 7.27 (d, $J=2.0$ Hz, 1H), 7.21 (d, $J=8.3$ Hz, 2H), 7.13 (dd, $J=2.5, 8.3$ Hz, 1H), 6.95 (dt, $J=2.5, 8.3$ Hz, 1H), 6.62 (t, $J=5.1$ Hz, 1H), 6.06 (d, $J=2.3$ Hz, 1H), 5.26 (s, 2H), 4.66 (d, $J=6.1$ Hz, 2H), 2.28 ppm (s, 3H); ^{13}C NMR (101 MHz, CDCl_3): $\delta=166.9, 161.9$ (d, $J=250.3$ Hz, 1C), 149.2, 140.8, 134.3 (d, $J=10.2$ Hz, 1C), 133.6, 131.6–131.5 (m, 1C), 131.6 (d, $J=8.0$ Hz, 1C), 130.2, 127.5 (s, 2C), 127.4 (s, 2C), 117 (d, $J=24.9$ Hz, 1C), 114.3 (d, $J=21.2$ Hz, 1C), 105.8, 55.1, 41.4, 13.6 ppm; LC–MS: $t_{\text{R}}=3.67$ min, m/z 358.09 $[M+H]^+$; purity: >95%.

***N*-[(2-chloro-4-fluorophenyl)methyl]-4-(1*H*-pyrazol-1-yl)methylbenzamide (26).** 1*H*-Pyrazole (27.2 mg, 0.4 mmol) was added following the procedure described for compound **25** to yield the title compound as a white solid. ^1H NMR (400 MHz, $[\text{D}_6]\text{DMSO}$): $\delta=9.00$ (t, $J=5.7$ Hz, 1H), 7.88–7.81 (m, 3H), 7.47 (d, $J=1.8$ Hz, 1H), 7.44 (dd, $J=2.5, 8.8$ Hz, 1H), 7.37 (dd, $J=6.3, 8.6$ Hz, 1H), 7.27 (d, $J=8.3$ Hz, 2H), 7.18 (dt, $J=2.8, 8.6$ Hz, 1H), 6.28 (t, $J=2.0$ Hz, 1H), 5.39 (s, 2H), 4.48 ppm (d, $J=5.6$ Hz, 2H); ^{13}C NMR (101 MHz, $[\text{D}_6]\text{DMSO}$): $\delta=166.1, 160.9$ (d, $J=246.6$ Hz, 1C), 141.1, 139.2, 133.2, 132.7 (d, $J=3.7$ Hz, 1C), 132.6 (d, $J=11.0$ Hz, 1C), 130.3, 130.1 (d, $J=9.5$ Hz, 1C), 127.5 (s, 2C), 127.3 (s, 2C), 116.4 (d, $J=24.9$ Hz, 1C), 114.2 (d, $J=21.2$ Hz, 1C), 105.5, 54.2, 40.1 ppm; LC–MS: $t_{\text{R}}=1.16$ min, m/z 343.09 $[M+H]^+$; purity: >95%.

***N*-[(2-chloro-4-fluorophenyl)methyl]-3-[(3,5-dimethyl-1*H*-pyrazol-1-yl)methyl]benzamide (27).** To a solution of 3,5-dimethyl-1*H*-pyrazole (41.8 mg, 0.43 mmol) and Na^tBuO (83.6 mg, 0.87 mmol) in DMF (1 mL) was slowly added another solution containing 3-(bromomethyl)benzoic acid (93.5 mg, 0.43 mmol) in DMF (1 mL); this was left to stir at room temperature for 2 h. The solvent was removed under vacuum, and the residue was dissolved in H_2O and then acidified to pH 6 with 2*N* HCl. It was then extracted with EtOAc (3×100 mL). The combined extracts were dried over MgSO_4 , filtered off, and the volatiles were removed under vacuum to afford 88 mg of the intermediate 3-(3,5-dimethyl-1*H*-pyrazol-1-yl)benzoic acid (88%). ^1H NMR (400 MHz, $[\text{D}_6]\text{DMSO}$): $\delta=9.04$ (t, $J=5.7$ Hz, 1H), 7.79 (d, $J=7.8$ Hz, 1H), 7.68 (s, 1H), 7.49–7.40 (m, 2H), 7.38 (dd, $J=6.3, 8.6$ Hz, 1H), 7.23–7.16 (m, 2H), 5.85 (s, 1H), 5.23 (s, 2H), 4.48 (d, $J=5.8$ Hz, 2H), 2.15 (s, 3H), 2.08 ppm (s, 3H); ^{13}C NMR (101 MHz, $[\text{D}_6]\text{DMSO}$): $\delta=166.2, 160.9$ (d, $J=245.9$ Hz, 1C), 146.1, 138.8, 138.3, 134.2, 132.7 (d, $J=3.7$ Hz, 1C), 132.5, 130.2 (d, $J=8.8$ Hz, 1C), 129.8, 128.6, 126., 126, 116.4 (d, $J=25.6$ Hz, 1C), 114.2 (d, $J=20.5$ Hz, 1C), 105.1, 51.3, 40, 13.3, 10.7 ppm; LC–MS: $t_{\text{R}}=1.22$ min, m/z 371.12 $[M+H]^+$; purity: >95%.

***N*-[(2-chloro-4-fluorophenyl)methyl]-4-[2-(3,5-dimethyl-1*H*-pyrazol-1-yl)ethyl]benzamide (28).** A solution of 3,5-dimethyl-1*H*-pyrazole (146.8 mg, 1.52 mmol), 4-(2-bromoethyl)benzoic acid (350 mg, 1.52 mmol), and NaHCO_3 (127 mg, 1.52 mmol) in MeOH (3 mL) was treated under microwave conditions at 135 °C for 2 h. The solvent was removed under vacuum, and the residue was dissolved in H_2O and then acidified to pH 7 with 1*N* HCl. It was then extracted with EtOAc (3×10 mL). The combined extracts were dried over MgSO_4 , filtered off, and the volatiles were removed under vacuum to afford 100 mg of the intermediate 4-(2-(3,5-dimethyl-1*H*-pyrazol-1-yl)ethyl)benzoic acid as a white solid (26%). 4-(2-(3,5-Dimethyl-1*H*-pyrazol-1-yl)ethyl)benzoic acid (100 mg, 0.4 mmol) and 2-chloro-4-fluorophenylmethanamine (77.6 mg, 0.45 mmol) were dissolved in DMF (5 mL) and reacted following the procedure described for compound **25** to yield 50 mg of the title compound as a white solid (35%). ^1H NMR (400 MHz, $[\text{D}_6]\text{DMSO}$): $\delta=8.96$ (t, $J=5.7$ Hz, 1H), 7.79 (d, $J=8.1$ Hz, 2H), 7.43 (dd, $J=2.7, 8.7$ Hz, 1H), 7.38 (dd, $J=6.2, 8.7$ Hz, 1H), 7.24–7.15 (m, 3H), 5.70 (s, 1H), 4.48 (d, $J=5.8$ Hz, 2H), 4.12 (t, $J=7.1$ Hz, 2H), 3.04 (t, $J=7.2$ Hz, 2H), 2.08 (s, 3H), 1.91 ppm (s, 3H); ^{13}C NMR (101 MHz, $[\text{D}_6]\text{DMSO}$): $\delta=166.1,$

160.8 (d, $J=245.9$ Hz, 1C), 145.7, 142.3, 138.5, 132.8 (d, $J=2.9$ Hz, 1C), 132.6 (d, $J=11.0$ Hz, 1C), 132, 130.2 (d, $J=8.8$ Hz, 1C), 128.8 (s, 2C), 127.3 (s, 2C), 116.3 (d, $J=25.6$ Hz, 1C), 114.2 (d, $J=21.2$ Hz, 1C), 104.2, 48.9, 40, 35.9, 13.4, 10.3 ppm; LC–MS: $t_{\text{R}}=1.23$ min, m/z 385.14 $[M+H]^+$; purity: >95%.

General procedure for the preparation of compounds 31, 33, 34, 36, and 37: methyl 4-((4-methylthiazol-2-yl)methyl)benzoate (29). To a suspension of Zn^0 (261 mg, 4 mmol) in THF (3 mL) at 100 °C under Ar atmosphere, methyl 4-(bromomethyl)benzoate (916 mg, 4 mmol) was added, and the mixture was left under stirring for 1.5 h. The mixture was allowed to reach room temperature, and a solution of 2-iodo-4-methylthiazole (300 mg, 1.5 mmol) and tetrakis(triphenylphosphine)palladium (462 mg, 0.4 mmol) in THF (4 mL) was added, holding the mixture at reflux for 3 h. Volatiles were removed under vacuum, and the crude was re-dissolved in EtOAc and washed with NaHCO_3 and brine. The organic layer was dried over MgSO_4 , and the volatiles were removed under vacuum. The resulting crude was purified by column chromatography to yield 126 mg of the title compound as a yellow oil (40%). ^1H NMR (300 MHz, CDCl_3): $\delta=8.00$ (d, $J=8.3$ Hz, 2H), 7.38 (d, $J=8.2$ Hz, 2H), 6.76 (d, $J=1.0$ Hz, 1H), 4.35 (s, 2H), 3.90 (s, 3H), 2.49–2.39 ppm (m, 3H).

4-((4-methylthiazol-2-yl)methyl)benzoic acid (30). To a solution of **29** (122 mg, 0.5 mmol) in THF (5 mL) was added dropwise a mixture of LiOH (24 mg, 1 mmol) in H_2O (5 mL), and the reaction was to stir at room temperature overnight. Volatiles were removed under vacuum, and the crude was re-dissolved in H_2O and acidified to pH 5 with HCl. The resulting precipitate was filtered off to yield 102 mg of the title compound as a brown solid (87%). ^1H NMR (300 MHz, CDCl_3): $\delta=8.06$ (d, $J=8.1$ Hz, 2H), 7.42 (d, $J=7.9$ Hz, 2H), 6.77 (s, 1H), 4.38 (s, 2H), 2.44 ppm (s, 3H).

***N*-[(2-chloro-4-fluorobenzyl)-4-((4-methylthiazol-2-yl)methyl)benzamide (31).** 2-Chloro-4-fluorophenylmethanamine (69 mg, 0.43 mmol) and compound **30** (100 mg, 0.43 mmol) were mixed following the procedure described for **22** to yield 40 mg of the title compound as a yellow solid (25%). ^1H NMR (400 MHz, CDCl_3): $\delta=7.74$ (d, $J=8.1$ Hz, 2H), 7.46 (dd, $J=5.9, 8.5$ Hz, 1H), 7.38 (d, $J=8.3$ Hz, 2H), 7.14 (dd, $J=2.5, 8.3$ Hz, 1H), 6.96 (dt, $J=2.7, 8.3$ Hz, 1H), 6.75 (d, $J=1.0$ Hz, 1H), 6.57 (s, 1H), 4.68 (d, $J=6.1$ Hz, 2H), 4.33 (s, 2H), 2.42 ppm (d, $J=1.0$ Hz, 3H); ^{13}C NMR (101 MHz, CDCl_3): $\delta=168.3, 167, 162$ (d, $J=250.3$ Hz, 1C), 152.6, 141.8, 134.3 (d, $J=11.0$ Hz, 1C), 132.9, 131.8, 131.6 (d, $J=8.8$ Hz, 1C), 129.3 (s, 2C), 127.4 (s, 2C), 116.8 (d, $J=24.9$ Hz, 1C), 114.3 (d, $J=21.2$ Hz, 1C), 113.6, 41.4, 39.4, 17.1 ppm; LC–MS: $t_{\text{R}}=1.24$ min, m/z 374.07 $[M+H]^+$; purity: >95%.

***N*-[(2-chloro-4-fluorophenyl)methyl]-4-(1,3-thiazol-2-yl)methylbenzamide (33).** Following the procedure described for compound **31** to obtain 4-(1,3-thiazol-2-yl)methylbenzoic acid, 2-chloro-4-fluorophenylmethanamine (220 mg, 1.2 mmol) and 4-(1,3-thiazol-2-yl)methylbenzoic acid (190 mg, 1.2 mmol) were mixed following the procedure described for **22** to yield 112 mg of the title compound as a white solid (26%). ^1H NMR (400 MHz, CDCl_3): $\delta=7.74$ (d, $J=8.1$ Hz, 2H), 7.71 (d, $J=3.3$ Hz, 1H), 7.45 (dd, $J=6.2, 8.5$ Hz, 1H), 7.38 (d, $J=8.1$ Hz, 2H), 7.22 (d, $J=3.3$ Hz, 1H), 7.13 (dd, $J=2.3, 8.3$ Hz, 1H), 6.96 (dt, $J=2.5, 8.3$ Hz, 1H), 6.58 (brs, 1H), 4.68 (d, $J=6.1$ Hz, 2H), 4.38 ppm (s, 2H); ^{13}C NMR (101 MHz, CDCl_3): $\delta=168.9, 167, 162$ (d, $J=250.3$ Hz, 1C), 142.7, 141.7, 134.3 (d, $J=11.0$ Hz, 1C), 133, 131.8, 131.7 (d, $J=8.8$ Hz, 1C), 129.3 (s, 2C), 127.5 (s, 2C), 119.2, 117 (d, $J=24.9$ Hz, 1C), 114.3 (d, $J=20.5$ Hz, 1C), 41.4, 39.2 ppm; LC–MS: $t_{\text{R}}=1.20$ min, m/z 360.05 $[M+H]^+$; purity: >95%.

***N*-[(2-chloro-4-fluorophenyl)methyl]-4-[(dimethyl-1,3-thiazol-2-yl)methyl]benzamide (34)**. Following the procedure described for compound **31** to obtain 4-[(dimethyl-1,3-thiazol-2-yl)methyl]benzoic acid, 2-chloro-4-fluorophenylmethanamine (27 mg, 0.14 mmol) and 4-[(dimethyl-1,3-thiazol-2-yl)methyl]benzoic acid (35 mg, 0.15 mmol) were mixed following the procedure described for **22** to yield 9 mg of the title compound as a white oil (17%). ¹H NMR (300 MHz, [D₆]DMSO): δ = 9.00 (t, *J* = 5.7 Hz, 1H), 7.85 (d, *J* = 8.2 Hz, 2H), 7.49–7.32 (m, 4H), 7.19 (dt, *J* = 2.6, 8.6 Hz, 1H), 4.49 (d, *J* = 5.7 Hz, 2H), 4.24 (s, 2H), 2.24 (s, 3H), 2.19 ppm (s, 3H); LC–MS: *t_R* = 2.86 min, *m/z* 380.08 [*M* + *H*]⁺; purity: > 95%.

***N*-[(2-chloro-4-fluorophenyl)methyl]-4-[(6-methylpyridin-2-yl)methyl]benzamide (36)**. Following the procedure described for compound **31** to obtain 4-[(6-methylpyridin-2-yl)methyl]benzoic acid, 2-chloro-4-fluorophenylmethanamine (52.6 mg, 0.33 mmol) and 4-[(6-methylpyridin-2-yl)methyl]benzoic acid (64 mg, 0.28 mmol) were mixed following the procedure described for **22** to yield 20 mg of the title compound as a yellow solid (20%). ¹H NMR (400 MHz, [D₆]DMSO): δ = 8.95 (t, *J* = 5.7 Hz, 1H), 7.82 (d, *J* = 8.3 Hz, 2H), 7.58 (t, *J* = 7.7 Hz, 1H), 7.43 (dd, *J* = 2.5, 8.8 Hz, 1H), 7.39–7.33 (m, 3H), 7.18 (dt, *J* = 2.7, 8.5 Hz, 1H), 7.09–7.02 (m, 2H), 4.48 (d, *J* = 5.6 Hz, 2H), 4.08 (s, 2H), 2.42 ppm (s, 3H); ¹³C NMR (101 MHz, [D₆]DMSO): δ = 166.2, 160.9 (d, *J* = 259.8 Hz, 1C), 159.3, 157.4, 143.5, 136.9, 132.8 (d, *J* = 3.7 Hz, 1C), 131.9, 130.1 (d, *J* = 9.5 Hz, 2C), 128.8 (s, 2C), 127.4 (s, 2C), 120.7, 120, 116.3 (d, *J* = 24.9 Hz, 1C), 114.2 (d, *J* = 21.2 Hz, 1C), 43.5, 40, 24 ppm; LC–MS: *t_R* = 1.23 min, *m/z* 368.11 [*M* + *H*]⁺; purity: > 95%.

***N*-[(2-chloro-4-fluorophenyl)methyl]-4-[(6-(trifluoromethyl)pyridin-2-yl)methyl]benzamide (37)**. Following the procedure described for compound **31** to obtain 4-[(6-(trifluoromethyl)pyridin-2-yl)methyl]benzoic acid, 2-chloro-4-fluorophenylmethanamine (33.5 mg, 0.21 mmol) and 4-[(6-(trifluoromethyl)pyridin-2-yl)methyl]benzoic acid (40 mg, 0.14 mmol) were mixed following the procedure described for **22** to yield 20 mg of the title compound as a white solid (35%). ¹H NMR (300 MHz, [D₆]DMSO): δ = 8.98 (t, *J* = 5.8 Hz, 1H), 8.01 (t, *J* = 7.8 Hz, 1H), 7.84 (d, *J* = 8.3 Hz, 2H), 7.74 (d, *J* = 7.6 Hz, 1H), 7.61 (d, *J* = 7.9 Hz, 1H), 7.47–7.31 (m, 4H), 7.18 (dt, *J* = 2.7, 8.6 Hz, 1H), 4.47 (d, *J* = 5.7 Hz, 2H), 4.25 ppm (s, 2H); LC–MS: *t_R* = 3.65 min, *m/z* 422.08 [*M* + *H*]⁺; purity: > 95%.

4-[(2-methyl-1,3-thiazol-4-yl)methyl]benzonitrile (38). Pd(Ph₃)₄ (76 mg, 0.07 mmol) was added to a solution of (4-cyanophenyl)boronic acid (0.2 g, 1.36 mmol), 4-(chloromethyl)-2-methylthiazole (0.25 g, 0.36 mmol) and Na₂CO₃ (2 M, 3.4 mL, 6.8 mmol) in DME (6 mL) previously bubbled with N₂. The mixture was heated at 90 °C overnight. DME was evaporated, and the resulting crude was re-dissolved in EtOAc and washed with H₂O. The organic layer was dried over MgSO₄, and the volatiles were removed under vacuum. The resulting crude was purified by column chromatography to yield 0.17 g of the title compound as a colorless oil (59%). ¹H NMR (300 MHz, CDCl₃): δ = 7.65–7.54 (m, *J* = 8.2 Hz, 2H), 7.41–7.31 (m, *J* = 8.3 Hz, 2H), 6.71 (s, 1H), 4.13 (s, 2H), 2.69 ppm (s, 3H).

4-[(2-methyl-1,3-thiazol-4-yl)methyl]benzoic acid (39). A 5 N solution of KOH was added to a solution of compound **38** (0.17 g, 0.8 mmol) in EtOH (5 mL). The mixture was left under stirring at room temperature overnight. EtOH was evaporated, and the aqueous solution was extracted with *t*BuOMe. The aqueous layer was then acidified to pH 5 with 2 M HCl. The white precipitate was filtered off and washed with H₂O to obtain 0.11 g of the title compound (62%). ¹H NMR (300 MHz, CDCl₃): δ = 8.02–7.90 (m, 2H), 7.34–7.27 (m, 2H), 6.65 (s, 1H), 4.16–4.03 (m, 2H), 2.71–2.60 ppm (m, 3H).

***N*-[(2-chloro-4-fluorophenyl)methyl]-4-[(2-methyl-1,3-thiazol-4-yl)methyl]benzamide (32)**. 2-Chloro-4-fluorophenylmethanamine (80 mg, 0.46 mmol) and compound **39** (110 mg, 0.46 mmol) were mixed following the procedure described for **22** to yield 70 mg of the title compound as a white solid (40%). ¹H NMR (400 MHz, CDCl₃): δ = 7.76 (d, *J* = 8.3 Hz, 2H), 7.50 (dd, *J* = 6.1, 8.6 Hz, 1H), 7.37 (d, *J* = 8.1 Hz, 2H), 7.17 (dd, *J* = 2.5, 8.3 Hz, 1H), 7.00 (dt, *J* = 2.7, 8.3 Hz, 1H), 6.68 (s, 1H), 6.61 (t, *J* = 5.3 Hz, 1H), 4.72 (d, *J* = 6.1 Hz, 2H), 4.15 (s, 2H), 2.72 ppm (s, 3H); ¹³C NMR (101 MHz, CDCl₃): δ = 167.1, 166.1, 161.9 (d, *J* = 249.6 Hz, 1C), 154.8, 143.2, 134.3, 132.2, 131.7, 131.7–131.6 (m, 1C), 129.2 (s, 2C), 127.2 (s, 2C), 116.9 (d, *J* = 24.9 Hz, 1C), 114.3–114.1 (m, 1C), 114.2 (d, *J* = 32.9 Hz, 1C), 41.4, 37.6, 19.2 ppm; LC–MS: *t_R* = 1.24 min, *m/z* 374.07 [*M* + *H*]⁺; purity: > 95%.

***N*-[(2-chloro-4-fluorophenyl)methyl]-4-[(6-methylpyridin-2-yl)amino]benzamide (41)**. 6-Methyl-2-bromopyridine (14 μL, 0.11 mmol), compound **40** (30 mg, 0.11 mmol; Supporting Information), Pd₂(dba)₃ (4 mg, 0.004 mmol), dppp (3.7 mg, 0.008 mmol), and *n*BuO (15 mg, 1.5 mmol) were dissolved in toluene (3 mL). The mixture was purged with Ar and left under stirring at 75 °C overnight. H₂O and *t*BuOMe were added. The organic layer was dried over MgSO₄, and the volatiles were removed under vacuum. The resulting crude was purified by column chromatography to yield 19 mg of the title compound as a yellow solid (53%). ¹H NMR (400 MHz, CDCl₃): δ = 7.78–7.70 (m, 2H), 7.50–7.43 (m, 2H), 7.43–7.37 (m, 2H), 7.14 (dd, *J* = 2.5, 8.3 Hz, 1H), 6.96 (dt, *J* = 2.7, 8.3 Hz, 1H), 6.80 (s, 1H), 6.74 (d, *J* = 8.3 Hz, 1H), 6.69 (d, *J* = 7.3 Hz, 1H), 6.53 (t, *J* = 5.4 Hz, 1H), 4.68 (d, *J* = 6.1 Hz, 2H), 2.47 ppm (s, 3H); ¹³C NMR (101 MHz, CDCl₃): δ = 166.8, 161.9 (d, *J* = 249.6 Hz, 1C), 157.2, 153.9, 144.1, 138.3, 134.3 (d, *J* = 10.2 Hz, 1C), 131.9 (d, *J* = 3.7 Hz, 1C), 131.6 (d, *J* = 8.8 Hz, 1C), 128.4 (s, 2C), 126.8, 117.8 (s, 2C), 116.9 (d, *J* = 24.9 Hz, 1C), 115.5, 114.3 (d, *J* = 20.5 Hz, 1C), 106.6, 41.3, 24.1 ppm; LC–MS: *t_R* = 1.27 min, *m/z* 369.10 [*M* + *H*]⁺; purity: > 95%.

***N*-[(2-chloro-4-fluorophenyl)methyl]-4-[(6-methylpyridin-2-yl)oxy]benzamide (42)**. Compound **61** (100 mg, 0.36 mmol; Supporting Information) was dissolved in DMSO (4 mL), and NaH (60% oil suspension, 16 mg, 0.4 mmol) and finally 2-bromo-6-methylpyridine (74 mg, 0.43 mmol) were added; the resulting mixture was left to stir at 120 °C overnight. EtOAc and H₂O were then added. The organic layer was dried over Na₂SO₄, and volatiles were removed under vacuum. The resulting crude was purified by column chromatography to yield 20 mg of the title compound as an orange solid (20%). ¹H NMR (300 MHz, CDCl₃): δ = 7.94–7.71 (m, 2H), 7.59 (t, *J* = 7.7 Hz, 1H), 7.46 (dd, *J* = 6.1, 8.6 Hz, 1H), 7.23–7.09 (m, 3H), 7.07–6.87 (m, 2H), 6.68 (d, *J* = 8.2 Hz, 2H), 4.68 (d, *J* = 6.0 Hz, 2H), 2.44 ppm (s, 3H); LC–MS: *t_R* = 2.95 min, *m/z* 370.09 [*M* + *H*]⁺; purity: > 95%.

***N*-[(2-chloro-4-fluorophenyl)methyl]-4-[(6-methylpyridin-2-yl)sulfonyl]benzamide (43)**. Compound **62** (70 mg, 0.24 mmol; Supporting Information), K₂CO₃ (99 mg, 0.72 mmol) and 2-bromo-6-methylpyridine (0.03 mL, 0.24 mmol) were dissolved in DMF (5 mL) and heated at 170 °C 5 h. DMF was removed under high vacuum, and the resulting crude was re-dissolved in EtOAc and washed with H₂O. The organic layer was dried over Na₂SO₄, and volatiles were removed under vacuum. The resulting crude was purified by column chromatography to yield 28 mg of the title compound as a white solid (50%). ¹H NMR (300 MHz, [D₆]DMSO): δ = 7.76 (d, *J* = 8.2 Hz, 2H), 7.57 (d, *J* = 8.2 Hz, 2H), 7.47 (dd, *J* = 6.0, 8.5 Hz, 1H), 7.39 (t, *J* = 7.8 Hz, 1H), 7.14 (dd, *J* = 2.6, 8.3 Hz, 1H), 7.04–6.87 (m, 2H), 6.78 (d, *J* = 7.9 Hz, 1H), 6.65 (t, *J* = 5.4 Hz, 1H), 4.69 (d, *J* =

6.0 Hz, 2H), 2.51 ppm (s, 3H); LC-MS: t_R = 2.99 min, m/z 386.07 $[M+H]^+$; purity: > 95%.

***N*-[(2-chloro-4-fluorophenyl)methyl]-4-[(6-methylpyridin-2-yl)-oxy]methyl]benzamide (44).** Compound **63** (100 mg, 0.28 mmol; Supporting Information), Cs_2CO_3 (182 mg, 0.56 mmol), and 6-methylpyridine-2-ol (30 mg, 0.28 mmol) were dissolved in CH_3CN (5 mL) and heated at 60 °C for 2 h. The solvent was removed under vacuum, and the resulting crude was re-dissolved in EtOAc and washed with H_2O . The organic layer was dried over Na_2SO_4 and volatiles were removed under vacuum. The resulting crude was purified by column chromatography to yield 45 mg of the title compound as a yellow solid (42%). ^1H NMR (400 MHz, CDCl_3): δ = 7.77 (d, J = 8.1 Hz, 2H), 7.52 (d, J = 8.1 Hz, 2H), 7.50–7.41 (m, 2H), 7.14 (dd, J = 2.7, 8.5 Hz, 1H), 6.97 (dt, J = 2.7, 8.3 Hz, 1H), 6.73 (d, J = 7.3 Hz, 1H), 6.59 (d, J = 8.3 Hz, 2H), 5.41 (s, 2H), 4.69 (d, J = 6.1 Hz, 2H), 2.44 ppm (s, 3H); ^{13}C NMR (101 MHz, CDCl_3): δ = 167.1, 162.7, 162.2 (d, J = 248.8 Hz, 1C), 156.2, 141.7, 138.9, 134.3 (d, J = 10.2 Hz, 1C), 133.3, 131.7 (d, J = 3.7 Hz, 1C), 131.6 (d, J = 8.8 Hz, 1C), 127.9, 127, 117 (d, J = 24.9 Hz, 1C), 116.1, 114.3 (d, J = 21.2 Hz, 1C), 107.5, 66.5, 41.4, 24.0 ppm; LC-MS: t_R = 1.35 min, m/z 384.10 $[M+H]^+$; purity: > 95%.

***N*-[(2-chloro-4-fluorophenyl)methyl]-4-[2-(6-methylpyridin-2-yl)-ethyl]benzamide trifluoroacetic salt (45).** Compound **61** (78 mg, 0.2 mmol; Supporting Information) was dissolved in MeOH (10 mL) containing 2 drops of HCl 2M. Then Pd/C (7.8 mg, 10% wt) was added, and the mixture was left under H_2 (3500 kPa) with stirring overnight. The mixture was filtered off to remove palladium under N_2 atmosphere. The volatiles were removed under vacuum, and the corresponding crude was purified by preparative HPLC to afford 30 mg of the title compound as a white solid (40%). ^1H NMR (300 MHz, CD_3OD): δ = 8.33 (t, J = 7.9 Hz, 1H), 7.88–7.76 (m, J = 8.2 Hz, 2H), 7.76–7.62 (m, 2H), 7.41 (dd, J = 6.2, 8.6 Hz, 1H), 7.36–7.29 (m, J = 8.2 Hz, 2H), 7.24 (dd, J = 2.6, 8.7 Hz, 1H), 7.05 (dt, J = 2.5, 8.4 Hz, 1H), 4.61 (s, 2H), 3.21–3.13 (m, 2H), 2.74 ppm (s, 3H); LC-MS: t_R = 1.96 min, m/z 382.12 $[M+H]^+$; purity: > 95%.

***N*-[(2-chloro-4-fluorophenyl)methyl]-4-[(6-methylpyridin-2-yl)-sulfonyl]methyl]benzamide (46).** Compound **63** (284 mg, 0.8 mmol; Supporting Information) and 6-methylpyridine-2-thiol (100 mg, 0.8 mmol) were mixed following the same procedure described for **44** to yield 200 mg of the title compound as a white solid (62%). ^1H NMR (400 MHz, $[\text{D}_6]\text{DMSO}$): δ = 8.97 (t, J = 5.7 Hz, 1H), 7.81 (d, J = 8.3 Hz, 2H), 7.55–7.48 (m, 3H), 7.43 (dd, J = 2.5, 8.8 Hz, 1H), 7.37 (dd, J = 6.3, 8.6 Hz, 1H), 7.18 (dt, J = 2.7, 8.5 Hz, 1H), 7.07 (d, J = 7.8 Hz, 1H), 6.96 (d, J = 7.6 Hz, 1H), 4.47 (d, J = 5.6 Hz, 2H), 4.43 (s, 2H), 2.45 ppm (s, 3H); ^{13}C NMR (101 MHz, $[\text{D}_6]\text{DMSO}$): δ = 166.1, 160.9 (d, J = 245.9 Hz, 1C), 157.9, 156.5, 142.1, 137.0, 132.7 (d, J = 3.7 Hz, 1C), 132.5 (d, J = 9.5 Hz, 1C), 130.1 (d, J = 8.8 Hz, 1C), 128.9 (s, 2C), 127.3 (s, 2C), 119.2, 118.6, 116.3 (d, J = 24.9 Hz, 1C), 114.2 (d, J = 20.5 Hz, 1C), 40, 32.7, 24 ppm; LC-MS: t_R = 1.34 min, m/z 400.08 $[M+H]^+$; purity: > 95%.

2-(2-chloro-4-fluorophenyl)-*N*-(4-((3,5-dimethyl-1*H*-pyrazol-1-yl)-methyl)phenyl)acetamide (47). Compound **65** (100 mg, 0.49 mmol; Supporting Information) was dissolved in DMF (5 mL) and 2-chloro-4-fluorophenylacetic acid (101 mg, 0.54 mmol), HOBt (82 mg, 0.54 mmol), and EDCI (103 mg, 0.54 mmol) were added leaving the mixture under stirring at room temperature overnight. DMF was removed under high vacuum, and the resulting crude was purified by HPLC to afford 65 mg of the title compound as a white solid (36%). ^1H NMR (400 MHz, $[\text{D}_6]\text{DMSO}$): δ = 10.21 (s, 1H), 7.51 (d, J = 8.6 Hz, 2H), 7.47–7.39 (m, 2H), 7.19 (dt, J = 2.7, 8.5 Hz, 1H), 7.03 (d, J = 8.6 Hz, 2H), 5.82 (s, 1H), 5.10 (s, 2H), 3.79

(s, 2H), 2.13 (s, 3H), 2.07 ppm (s, 3H); ^{13}C NMR (101 MHz, $[\text{D}_6]\text{DMSO}$): δ = 167.7, 162.6–159.2 (m, 1C), 145.8, 138.5, 138.2, 134.3 (d, J = 11.0 Hz, 1C), 133.4 (d, J = 8.8 Hz, 1C), 132.5, 130.3 (d, J = 3.7 Hz, 1C), 127.4 (s, 2C), 119.1 (s, 2C), 116.2 (d, J = 24.9 Hz, 1C), 114.1 (d, J = 21.2 Hz, 1C), 104.9, 51.2, 40.2, 13.3, 10.6 ppm; LC-MS: t_R = 1.22 min, m/z 371.12 $[M+H]^+$; purity: > 95%.

Biology

In vitro assays

***InhA* enzyme assay.** Four assays were carried out for each compound, and reported data are the mean values. Enzyme activity was measured fluorimetrically by following NADH oxidation (λ_{ex} = 340 nm, λ_{em} = 480 nm) using 50 μM NADH and 50 μM 2-*trans*-dodecenoyl-CoA (DDCoA) as substrates. Dose–response experiments to determine IC_{50} values were performed using 5 nM *InhA*; percent remaining enzyme activity (%AR) at various compound concentrations were calculated with the formula: %AR = $100 \times \{(\text{sample} - \text{ctrl}_2) / (\text{ctrl}_1 - \text{ctrl}_2)\}$, for which *sample* is the enzyme activity for each compound concentration, ctrl_1 is enzyme activity in the absence of test compound, and ctrl_2 is NADH oxidation in the absence of enzyme. IC_{50} values were calculated by fitting %AR to a two-parameter equation: %AR = $100 / \{1 + ([\text{compd}] / \text{IC}_{50})^s\}$, in which *s* is a slope factor; IC_{50} values were calculated using GraFit software (ver. 5.0.12, Erithacus Software Ltd.). All reactions were performed in 30 mM PIPES buffer (pH 6.8) at 25 °C.

***InhA* enzyme assay (high-throughput screening methodology).** Compounds **3–8**, **10–13**, **25**, **26**, **31**, and **55** were evaluated following this methodology. Two assays were carried out for each compound, and reported data are the mean values. Enzyme activity was measured fluorimetrically by monitoring NADH oxidation either directly (λ_{ex} = 340 nm, λ_{em} = 480 nm), or by coupling with the generation of resorufin (λ_{ex} = 550 nm, λ_{em} = 590 nm) with diaphorase.^[30] Dose–response experiments to determine IC_{50} values were performed using 50 μM NADH and 50 μM 2-*trans*-dodecenoyl-CoA (DDCoA) as substrates, and 5 nM *InhA*. Percent remaining enzyme activity (%AR) at various compound concentrations were calculated with the formula: %AR = $100 \times \{(\text{sample} - \text{ctrl}_2) / (\text{ctrl}_1 - \text{ctrl}_2)\}$, for which *sample* is the enzyme activity for each compound concentration, ctrl_1 is enzyme activity in the absence of test compound, and ctrl_2 is NADH oxidation in the absence of enzyme. IC_{50} values were calculated using GraFit software (ver. 5.0.12, Erithacus Software Ltd.) and ActivityBase software (ver. 7.4.5.2). All reactions were run in 30 mM PIPES buffer (pH 6.8) and 0.1 mg mL^{-1} BSA at 25 °C.

MIC_{90} determination on mycobacteria. For each compound the average value of duplicate determinations was calculated. We considered the duplicates to be correct if they were in the range of ± 1 dilution (1:2) in the assay. Minimum inhibitory concentration (MIC_{90}) values against *M. tuberculosis* strains for each compound tested were determined in 96-well flat-bottom polystyrene microtiter plates in a final volume of 100 μL . Ten twofold drug dilutions in neat DMSO starting at 50 mM were performed. Drug solutions were added to Middlebrook 7H9 medium (Difco), and isoniazid (INH; Sigma–Aldrich) was used as a positive control with twofold dilutions of INH starting at 160 $\mu\text{g mL}^{-1}$. The inoculums were standardized to $\sim 1 \times 10^7$ CFU mL^{-1} and diluted 1:100 in Middlebrook 7H9 broth. The inoculums (100 μL each) were added to the entire plate, but wells G12 and H12 were used as blank controls. All plates were placed in a sealed box to prevent drying of the peripheral wells and incubated at 37 °C without shaking for six days. A resazurin so-

lution was prepared by dissolving one tablet of resazurin (*Resazurin Tablets for Milk Testing*, Ref. 330884Y, VWR Intl. Ltd.) in 30 mL sterile phosphate-buffered saline (PBS). Of this solution, 25 μL were added to each well. Fluorescence was measured after 48 h ($\lambda_{\text{ex}} = 530 \text{ nm}$, $\lambda_{\text{em}} = 590 \text{ nm}$; Spectramax M5, Molecular Devices) to determine MIC_{90} values.

General antimicrobial activity assay: Whole-cell antimicrobial activity was determined by broth microdilution using the Clinical and Laboratory Standards Institute (CLSI) recommended procedure, Document M7A7, "Methods for Dilution Susceptibility Tests for Bacteria that Grow Aerobically". Some compounds were evaluated against a panel of Gram-positive and Gram-negative organisms, including *Streptococcus aureus*, *Enterococcus faecalis*, *Haemophilus influenzae*, *Moraxella catarrhalis*, *Streptococcus pneumoniae*, and *Escherichia coli*. The MIC_{90} value was determined as the lowest compound concentration required to produce a $>80\%$ decrease in observed fluorescence.

InhA overexpression studies. Overexpression of the target has been shown to be a robust way to confirm the mode of action of antimicrobial agents. To establish a link between enzymatic and whole-cell activities, we cloned *Mycobacterium smegmatis* and *Mycobacterium tuberculosis inhA* genes under control of the acetamidase promoter. *M. smegmatis* transformants overexpressed InhA protein in the presence of acetamide, whereas *Mycobacterium bovis* BCG constitutively overexpress the target. In both species we observed a clear correlation between InhA expression and isoniazid sensitivity. Therefore, we have a whole-cell mode-of-action tool to determine if the predominant antitubercular effect of a new drug in *Mycobacterium* is via inhibition of InhA.

Microsomal fraction stability experiments. Pooled mouse liver microsomes were purchased from Xenotech (www.xenotech.com/home). Microsomes (final protein concentration: 0.5 mg mL^{-1}), MgCl_2 (5 mM final), and test compound (final substrate concentration: $0.5 \mu\text{M}$; final DMSO concentration: 0.5%) in 0.1 M phosphate buffer pH 7.4 were pre-incubated at 37°C prior to the addition of NADPH (final concentration: 1 mM) to initiate the reaction. The final incubation volume was 600 μL . All incubations were performed singularly for each test compound. Each compound was incubated for 30 min, and samples (90 μL) were taken at 0, 3, 6, 9, 12, 15, 18, 21, 24, 27, and 30 min. Reactions were stopped by the addition of sample to 200 μL $\text{CH}_3\text{CN}/\text{MeOH}$ (3:1) containing an internal standard. The terminated samples were centrifuged at 3700 rpm for 15 min at 4°C to precipitate the protein. Quantitative analysis: following protein precipitation, the samples were analyzed using specific LC-MS/MS conditions. Data analysis: from a plot of $\ln[\text{peak area ratio}]$, i.e., (compound peak area)/(internal standard peak area) against time, the gradient of the line was determined. Subsequently, half-life ($t_{1/2}$) and intrinsic clearance (CL_{int}) were calculated using Equations (1)–(3) below:

$$\text{Elimination rate constant } (k) = (-\text{gradient}) \quad (1)$$

$$t_{1/2} [\text{min}] = 0.693/k \quad (2)$$

$$\text{CL}_{\text{int}} [\text{mL min}^{-1} \{\text{g protein}\}^{-1}] = V \times 0.693/t_{1/2} \quad (3)$$

in which V = incubation volume ($\text{mL}\{\text{g microsomal protein}\}^{-1}$). Human biological samples were sourced ethically, and their research use was in accord with the terms of the informed consent given by donors.

In vivo assays

All animal studies were ethically reviewed and carried out in accordance with European Directive 2010/63/EU and the GSK Policy on the Care, Welfare, and Treatment of Animals.

In vivo efficacy assay

Mice. C57BL/6 specific-pathogen-free (*spf*) six- to eight-week-old female mice were obtained from Harlan Iberica, (St. Feliu de Codines, Spain). They were shipped under suitable travel conditions, with the corresponding certificate of health and origin. All animals were kept under controlled conditions in a P3 high-security facility with sterile food and water ad libitum.

Bacteria and infection. The virulent *M. tuberculosis* strain H₃₇Rv Pasteur was grown to mid-log phase in Proskauer–Beck medium and stored at -70°C in 2 mL aliquots. Mice were placed in the exposure chamber of an airborne infection apparatus (Glas-col Inc., Terre Haute, IN, USA). The nebulizer compartment was filled with 7.5 mL of an *M. tuberculosis* suspension at a previously calculated concentration to provide an approximate uptake of 20 viable bacilli within the lungs.

Antibiotic formulations. Isoniazide was provided by Sigma (Madrid, Spain) and diluted in distilled water before administration. SB-713520 was formulated as a suspension in 1% methyl cellulose. The products were administered for two weeks (Monday–Friday) starting on day 11 after infection. The schedule was once daily for isoniazid and twice daily for SB-713520.

CFU determination. The number of viable bacteria in lung and spleen homogenates was measured at day 25 after infection by plating serial dilutions on nutrient Middlebrook 7H11 agar (Biomedics s.L., Madrid, Spain) and counting bacterial colony formation after incubation at 37°C . Special care was taken to exclude hilar lymph nodes at the time of lung removal in order to not artificially increase the CFU value. Lungs and spleen were immediately extracted after euthanasia.

Animal health. Animals were supervised every day under a protocol paying attention to weight loss, apparent good health (bristled hair and wounded skin) and behavior (signs of aggression or isolation). Animals were euthanized with halothane (Fluothane, Zeneca Farma) overdose so as to avoid suffering. Sentinel animals were used to determine *spf* conditions in the facility. Tests for 25 known pathogens were all negative. All experimental proceedings were approved and supervised by the Animal Care Committee of "German Trias i Pujol" University Hospital in agreement with the European Union Laws for protection of experimental animals.

Pharmacokinetics studies

C57BL/6 female mice of 18–20 g weight were used. Experimental compounds were administered by oral gavage at 500 mg kg^{-1} per single dose at a volume of 20 mL kg^{-1} ($n = 4$ mice per time point). All mice received treatment in the fed state. Compound was administered as a 1% methyl cellulose suspension. Peripheral total blood was the compartment chosen for the establishment of compound concentrations: aliquots of 25 μL of blood were taken by cardiac puncture for each mouse (euthanized by CO_2) at 15, 30, 40, 50 min, and 1, 1.5, 3, 6, and 8 h ($n = 4$ mice per time point). LC-MS was used as the analytical method for establishment of compound concentration in blood with a sensitivity of $1\text{--}5 \text{ ng mL}^{-1}$ (LLQ) in 25 μL blood. The non-compartmental data analysis (NCA) was performed with WinNonlin (ver. 5.2; Pharsight, Certara L.P.), and sup-

plementary analysis was performed with GraphPad Prism (ver. 5; GraphPad Software Inc.).

X-ray crystallography

InhA was cloned, expressed, and purified as described previously.^[31] The protein was incubated with 2 mM NAD⁺ and 2 mM compound **1** prior to crystallization. The complex crystallized in 14–24% PEG 3350 and 0.1 M *N*-(2-acetamido)iminodiacetic acid, pH 6.8, 6% DMSO, and 0.18 M ammonium sulfate at 20 °C. Data were collected to 2.2 Å resolution at beam line 23ID of the Advanced Photon Source, Argonne National Laboratory. The structure was solved by molecular replacement. Details and statistics are provided in the Supporting Information and at the RCSB Protein Data Bank (PDB ID: 4QXM).

Acknowledgements

The authors thank Daniel Álvarez for his help with the InhA biochemical assay; Ana Luisa Rodríguez, Katie Hudd, Alastair Roberts, Maria Cruz García Palancar at GSK-DDW Tres Cantos, and Matthew Wolfendale for their organic chemistry contributions; the Pharmacology Group at GSK Tres Cantos, Sophie Huss, and Oscar Atienza for *in vitro* DMPK studies; as well as Juan Miguel Siles at the Core Chemistry Group. We also thank the Global Alliance for TB Drug Development for providing funding for this investigation.

Keywords: antimycobacterials • benzamides • drug discovery • InhA • medicinal chemistry • tuberculosis

- [1] World Health Organization (WHO), Global Tuberculosis Report **2014**, ISBN: 9789241564809, apps.who.int/iris/bitstream/10665/137094/1/9789241564809_eng.pdf.
- [2] A. Rattan, A. Kalia, N. Ahmad, *Emerging Infect. Dis.* **1998**, *4*, 195–209.
- [3] M. C. Becerra, J. Bayona, J. Freeman, P. E. Farmer, J. Y. Kim, *Int. J. Tuberc. Lung Dis.* **2000**, *4*, 387–394.
- [4] C. Dye, M. A. Espinal, J. C. Watt, C. Mbiaga, B. G. Williams, *J. Infect. Dis.* **2002**, *185*, 1197–1202.
- [5] C. Y. Chiang, R. Centis, G. B. Migliori, *Respirology* **2010**, *15*, 413–432.
- [6] World Health Organization (WHO), Multidrug and Extensively Drug-Resistant TB (M/XDR-TB): Global Report on Surveillance and Response, **2010**, ISBN: 9789241599191, apps.who.int/iris/bitstream/10665/44286/1/9789241599191_eng.pdf?ua=1&ua=1.
- [7] R. Banerjee, G. F. Schechter, J. Flood, T. C. Porco, *Expert Rev. Anti-Infect. Ther.* **2008**, *6*, 713–724.
- [8] M. Berry, O. M. Kon, *Eur. Respir. Rev.* **2009**, *18*, 195–197.
- [9] World Health Organization (WHO), *What is DOTS? A Guide to Understanding the WHO-Recommended TB Control Strategy Known as DOTS*, Document WHO/CDS/CPC/TB/99.270, **1999**, apps.who.int/iris/bitstream/10665/65979/1/WHO_CDS_CPC_TB_99.270.pdf.
- [10] R. Mahajan, *Int. J. Appl. Basic Med. Res.* **2013**, *3*, 1–2.
- [11] C. Vilcheze, H. R. Morbidoni, T. R. Weisbrod, H. Iwamoto, M. Kuo, J. C. Sacchettini, W. R. Jacobs, *J. Bacteriol.* **2000**, *182*, 4059–4067.
- [12] A. Banerjee, E. Dubnau, A. Quemard, V. Balasubramanian, T. Wilson, D. Collins, G. de Lisle, W. R. Jacobs, Jr., *Science* **1994**, *263*, 227–230.
- [13] A. Dessen, A. Quemard, J. S. Blanchard, W. R. Jacobs, Jr., J. C. Sacchettini, *Science* **1995**, *267*, 1638–1641.
- [14] X. Y. Lu, Q. D. You, X. Chen, *Mini-Rev. Med. Chem.* **2010**, *10*, 182–192.
- [15] D. A. Rozwarski, G. A. Grant, H. D. Barton, W. R. Jacobs, Jr., J. C. Sacchettini, *Science* **1998**, *279*, 98–102.
- [16] L. Encinas, H. O'Keefe, M. Neu, M. J. Remuñán, A. M. Patel, A. Guardia, C. P. Davie, N. Pérez-Macías, H. Yang, M. A. Convery, J. A. Messer, E. Pérez-Herrán, P. A. Centrella, D. Álvarez-Gómez, M. A. Clark, S. Huss, G. K. O'Donovan, F. Ortega-Muro, W. McDowell, P. Castañeda, C. C. Arico-Muendel, S. Pajk, J. Rullás, I. Angulo-Barturen, E. Álvarez-Ruiz, A. Mendoza-Losana, L. L. Ballell Pages, J. Castro-Pichel, G. Evidar, *J. Med. Chem.* **2014**, *57*, 1276–1288.
- [17] J. Pan, P. J. Tonge, *Curr. Top. Med. Chem.* **2012**, *12*, 672–693.
- [18] X. Y. Lu, Q. D. You, Y. D. Chen, *Mini-Rev. Med. Chem.* **2010**, *10*, 181–192.
- [19] L. L. Ballell Pages, J. Castro-Pichel, R. Fernández, E. P. Fernandez, S. Gonzalez, M. L. Leon, A. Mendoza-Losana, M. J. Wolfendale (Glaxo Group Ltd.), Int. PCT Pub. No. WO2010118852 A1, **2010**.
- [20] J. Castro-Pichel, R. Fernandez, E. P. Fernandez, S. Gonzalez, A. Mallo (Glaxo Group Ltd.), Int. PCT Pub. No. WO2012049161 A1, **2012**.
- [21] U. H. Manjunatha, P. S. Rao, R. R. Kondreddi, C. G. Noble, L. R. Camacho, B. H. Tan, S. H. Ng, P. Shuyi, N. L. Ma, S. B. Lakshminarayana, M. Herve, S. W. Barnes, W. Yu, K. Kuhen, F. Blasco, D. Bee, J. R. Walker, P. J. Tonge, R. Glynn, P. W. Smith, T. T. Diagana, *Sci. Transl. Med.* **2015**, *7*, 269ra3.
- [22] Unpublished results.
- [23] E.-i. Negishi, Q. Hu, Z. Huang, M. Qian, G. Wang, *Aldrichimica Acta* **2005**, *38*(3), 71–88.
- [24] P. D. Leeson, B. Springthorpe, *Nat. Rev. Drug Discovery* **2007**, *6*, 881–890.
- [25] R. Young, D. V. Green, C. N. Luscombe, A. P. Hill, *Drug Discovery Today* **2011**, *16*, 822–830.
- [26] J. Bowes, A. J. Brown, J. Hamon, W. Jarolimek, A. Sridhar, G. Waldron, S. Whitebread, *Nat. Rev. Drug Discovery* **2012**, *11*, 909–922.
- [27] M. M. Hann, G. M. Keser, *Nat. Rev. Drug Discovery* **2012**, *11*, 355–365.
- [28] J. A. Arnott, S. L. Planey, *Expert Opin. Drug Discovery* **2012**, *7*, 863–875.
- [29] P. S. Shirude, P. Madhavapeddi, M. Naik, K. Murugan, V. Shinde, R. Nandishaiah, J. Bhat, A. Kumar, S. Hameed, G. Holdgate, G. Davies, H. McMiken, N. Hegde, A. Ambady, J. Venkatraman, M. Panda, B. Bandodkar, V. K. Sambandamurthy, J. A. Read, *J. Med. Chem.* **2013**, *56*, 8533–8542.
- [30] R. H. Batchelor, M. Zhou, *Anal. Biochem.* **2004**, *329*, 35–42.
- [31] J. S. Freundlich, F. Wang, C. Vilcheze, G. Gulten, R. Langley, G. A. Schiehsler, D. P. Jacobus, W. R. Jacobs, Jr., J. C. Sacchettini, *ChemMedChem* **2009**, *4*, 241–248.

Received: January 11, 2016

Revised: February 12, 2016

Published online on March 2, 2016